Published OnlineFirst April 13, 2010; DOI:10.1158/1078-0432.CCR-09-2214

Human Cancer Biology

Clinical Cancer Research

Combined Functional Genome Survey of Therapeutic Targets for Hepatocellular Carcinoma

Reiko Satow[1], Miki Shitashige[1], Yae Kanai[2], Fumitaka Takeshita[3], Hidenori Ojima[2], Takafumi Jigami[1], Kazufumi Honda[1], Tomoo Kosuge[4], Takahiro Ochiya[3], Setsuo Hirohashi[1,2], and Tesshi Yamada[1]

Abstract

Purpose: The outcome of patients with advanced hepatocellular carcinoma (HCC) has remained unsatisfactory. Patients with HCC suffer from chronic hepatitis or liver cirrhosis, and their reserve liver function is often limited.

Experimental Design: To develop new therapeutic agents that act specifically on HCC but interfere only minimally with residual liver function, we searched for genes that were upregulated in 20 cases of HCC [namely, discovery sets 1 (n = 10) and 2 (n = 10)] in comparison with corresponding nontumorous liver and a panel representing normal organs using high-density microarrays capable of detecting all exons in the human genome.

Results: Eleven transcripts whose expression was significantly increased in HCC were subjected to siRNA-based secondary screening of genes required for HCC cell proliferation as well as quantitative reverse transcription-PCR analysis [validation sets 1 (n = 20) and 2 (n = 44)] and immunohistochemistry (n = 19). We finally extracted four genes, *AKR1B10*, *HCAP-G*, *RRM2*, and *TPX2*, as candidate therapeutic targets for HCC. siRNA-mediated knockdown of these candidate genes inhibited the proliferation of HCC cells and the growth of HCC xenografts transplanted into immunodeficient mice.

Conclusions: The four genes we identified were highly expressed in HCC, and HCC cells are highly dependent on these genes for proliferation. Although many important genes must have been overlooked, the selected genes were biologically relevant. The combination of genome-wide expression and functional screening described here is a rapid and comprehensive approach that could be applied in the identification of therapeutic targets in any type of human malignancy. *Clin Cancer Res; 16(9); 2518–28. ©2010 AACR.*

Liver cancer is the fifth most common human cancer worldwide and the third most common cause of cancer mortality. Hepatocellular carcinoma (HCC) is the most common histologic subtype of liver cancer and is highly endemic in Southeast Asia and sub-Saharan Africa (1). HCC develops mainly in liver affected by chronic hepatitis or cirrhosis caused by persistent infection with hepatitis B or C virus; however, the precise molecular mechanisms that drive the transition from the background liver conditions to cancer are largely unknown. Liver resection, ethanol injection, radiofrequency ablation, and chemoembolization have been used successfully for the local management of HCC; however, no single cytotoxic chemotherapeutic agent has been proven effective for the systemic treatment of HCC; thus, the outcome for patients with locally advanced, multicentric, and/or metastatic HCC who are not eligible for these local treatments has remained unsatisfactory.

An increasing number of therapeutic agents targeting molecular components essential for cancer cell growth have begun to be incorporated into oncological practice: Imatinib, which blocks the Bcr-Abl fusion kinase of chronic myeloid leukemia (CML), is currently the first-line therapy for CML (2). The epidermal growth factor receptor inhibitors gefitinib and erlotinib have been used in the treatment of advanced non–small cell lung cancer (3). Recently, it was shown in a phase III study that sorafenib (BAY 43-9006), a multikinase inhibitor, significantly improved the overall survival of patients with advanced HCC (4, 5), and, consequently, sorafenib has since been approved for the treatment of patients with unresectable HCC by the American Food and Drug Administration. However, most patients enrolled in those studies retained relatively well-compensated

Authors' Affiliations: [1]Chemotherapy Division, [2]Pathology Division, and [3]Section for Studies on Metastasis, National Cancer Center Research Institute; and [4]Hepatobiliary and Pancreatic Surgery Division, National Cancer Center Hospital, Tokyo, Japan

Note: Supplementary data for this article are available at Clinical Cancer Research Online (http://clincancerres.aacrjournals.org/).

Microarray data from this study have been submitted to the Gene Expression Omnibus database (accession no. GSE12941).

Corresponding Author: Tesshi Yamada, Chemotherapy Division, National Cancer Center Research Institute, 5-1-1 Tsukiji, Chuo-ku, Tokyo 104-0045, Japan. Phone: 81-3-3542-2511; Fax: 81-3-3547-6045; E-mail: tyamada@ncc.go.jp.

doi: 10.1158/1078-0432.CCR-09-2214

Published OnlineFirst April 13, 2010; DOI:10.1158/1078-0432.CCR-09-2214

Translational Relevance

Liver cancer is the fifth most common human cancer worldwide and the third most common cause of cancer mortality. Recently, a multikinase inhibitor, sorafenib, has been approved as a systemic chemotherapeutic drug for advanced hepatocellular carcinoma (HCC); however, further improvement seems to be necessary. To identify an "Achilles heel" of HCC cells and develop new therapeutic agents that act specifically on HCC but interfere only minimally with residual liver function, we performed an unbiased survey of the whole genome. We finally identified four genes as candidates. siRNA-mediated knockdown of these candidate genes inhibited the proliferation of HCC cells and the growth of HCC xenografts transplanted into immunodeficient mice, confirming their feasibility as therapy targets.

liver function. In reality, the reserve liver function of HCC patients is often limited due to underlying liver conditions. Therefore, the safety and tolerability of sorafenib remain to be determined in HCC patients with compromised liver function. Therapeutic targeting molecules other than protein kinases have also been developed against various tumors of other organs (6–8). To identify a molecule essential for HCC cell growth and develop new therapeutic agents that would act specifically on HCC and only minimally interfere with residual liver function, a survey of the whole genome would be necessary.

In this study, we adopted a combined functional approach. We first searched for genes that were upregulated in HCC in comparison with the background nontumorous liver tissue. This was followed by siRNA-based screening of genes required for HCC cell proliferation. Recently, whole-genome RNA interference (RNAi)–based functional screening has been reported to successfully identify genes that sensitize lung cancer cells to a chemotherapeutic drug and genes required for proliferation and survival of several cancer cell lines; however, in those studies, the expressional specificity of the identified targets was not taken into consideration (9–12). Here, we report the identification of possible therapeutic target molecules of HCC through a combination of genome-wide expression and functional screening.

Materials and Methods

Patients and microarray analysis. Samples of HCC and surrounding nontumorous liver tissue were collected from 84 patients who underwent liver resection for HCC at the National Cancer Center Hospital (Tokyo, Japan) with informed consent. The clinical and histologic data for these patients are summarized in Supplementary Table S1. Total RNA of normal human organs was obtained from a commercial source (FirstChoice Human Total RNA Survey Panel, Ambion).

One microgram of total RNA was converted to end-labeled cRNA using a Whole Transcript Sense Target Labeling kit (Affymetrix). The fluorescent cRNA probes were hybridized to Human Exon 1.0 ST arrays (Affymetrix), as instructed by the supplier. Data analysis was carried out using the ArrayAssist software package (version 5.5.1, Stratagene). A GC content-based background correction followed by quantile normalization was done with an exonRMA algorithm available in the package. Multiple exonic expression data were also summarized into a single value using the same algorithm, as instructed by the supplier (http://www.stratagene.com/manuals/ArrayAssist.pdf).

The protocol of this study was reviewed and approved by the ethics committee of the National Cancer Center (Tokyo, Japan).

Cell lines. Three human cell lines derived from HCC were used in this study. KIM-1 was kindly provided by Dr. Masamichi Kojiro (Kurume University, Kurume, Japan). Hep3B was obtained from the Cell Resource Center for Biomedical Research, Tohoku University (Sendai, Japan). HLE was obtained from the Health Science Research Resources Bank (Osaka, Japan). KIM-1 and Hep3B were maintained in RPMI 1640 (Invitrogen) supplemented with 10% fetal bovine serum. HLE was maintained in Dulbecco's modified Eagle's medium (Invitrogen) supplemented with 10% fetal bovine serum.

siRNA-based functional screening. The day before siRNA transfection, cells were seeded at 5×10^3 per well in 96-well plates to obtain 50% to 60% confluency. They were then transfected with siRNA using Lipofectamine 2000 (Invitrogen) at a concentration of 10, 20, or 50 nmol/L in KIM1, Hep3B, or HLE cells, respectively. Three days later, the relative proportion of living cells was assessed using a Premix WST-1 Cell Proliferation Assay System (Takara Bio) in accordance with the manufacturer's instructions. The siRNA was synthesized by Ambion, and the identification (ID) numbers of siRNAs used in this study are listed in Supplementary Table S4. Silencer Negative Control #1 siRNA (Ambion) was used as a nontargeting control. siRNA targeting *TOP2A* was described previously (13).

Real-time PCR. First-strand cDNA was synthesized from 1 μg of total RNA using SuperScript reverse transcriptase (Invitrogen). Real-time PCR was done as described previously (14). Primers and probes sets were obtained from Applied Biosystems, and their Assay IDs are provided in Supplementary Table S5. The amplification reaction was done according to the manufacturer's instructions (95°C for 10 minutes followed by 40 cycles of 95°C for 15 seconds, 50°C for 2 minutes, and 60°C for 1 minute).

Immunohistochemistry and immunoblot analysis. Anti-AKR1B10 (clone 1A6) and anti–HCAP-G (clone 4B1) monoclonal antibodies were purchased from Abnova. Anti-RRM2 antibody (E-16) was purchased from Santa

Published OnlineFirst April 13, 2010; DOI:10.1158/1078-0432.CCR-09-2214

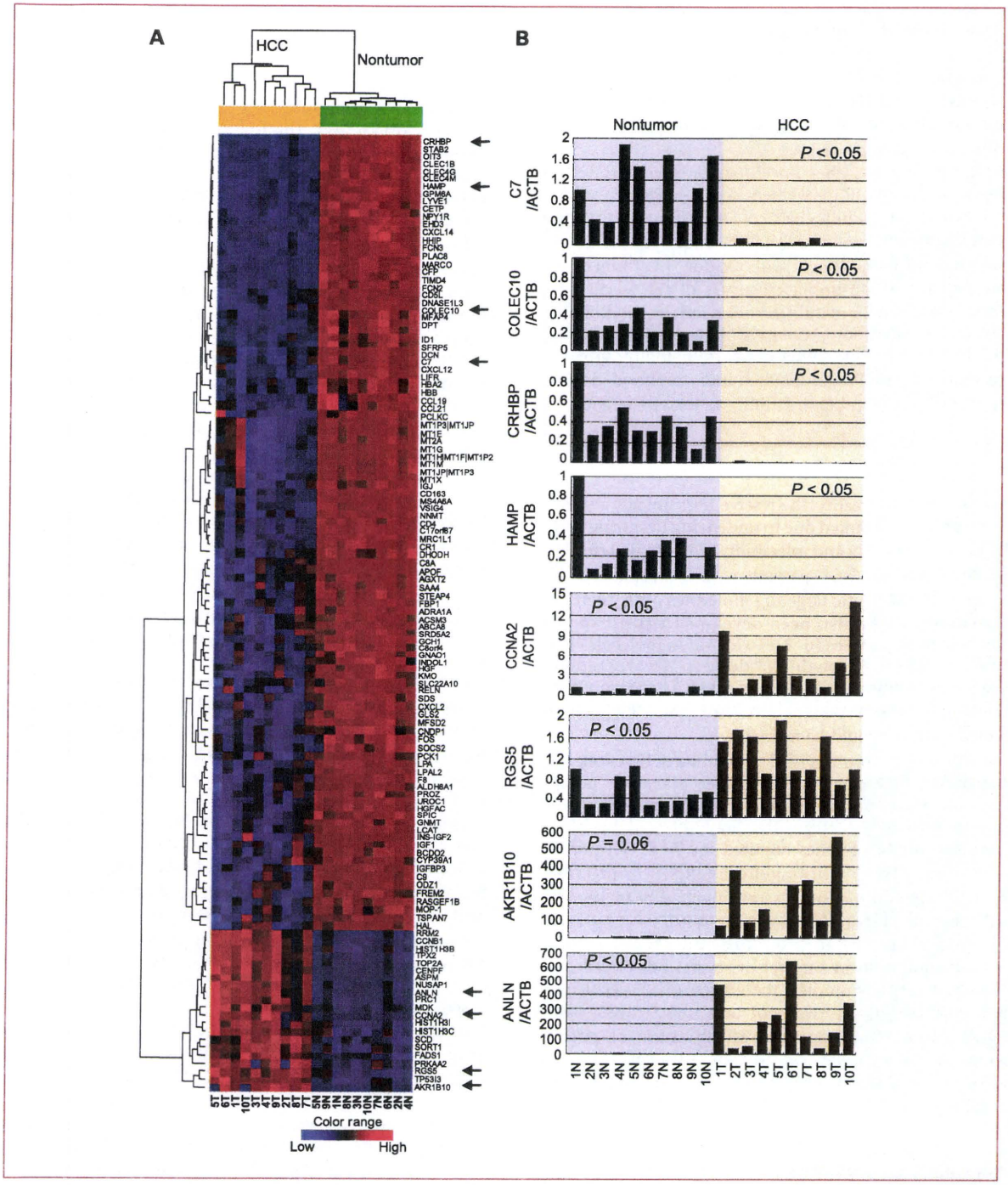

Fig. 1. Genes differentially expressed between HCC and nontumorous liver. A, hierarchical clustering of 124 genes whose expression differed significantly ($P < 0.001$ and >3-fold change) between HCC and adjacent nontumorous liver. Transcriptional signal intensity is shown as a heat map. Red indicates higher signals, whereas blue indicates lower signals. Arrows indicate eight genes selected for validation by real-time PCR (B). B, validation of the microarray data by real-time RT-PCR. The expression levels of eight representative genes whose expression differed significantly between adjacent nontumorous liver (left) and HCC (right) were validated by real-time RT-PCR (shown in arbitrary units). Significant correlation between array (discovery set 1) and real-time RT-PCR data was confirmed by calculating correlation coefficient values in eight randomly selected genes (indicated by arrows in A): *C7*, 0.96; *COLEC10*, 0.97; *CRHBP*, 0.98; *HAMP*, 0.98; *CCNA2*, 0.82; *RGS5*, 0.80; *AKR1B10*, 0.98; *ANLA*, 0.92. The significance of differential expression between HCC and adjacent nontumorous liver tissue was assessed using a permutation paired *t* test, and Bonferroni-corrected *P* values are provided.

Published OnlineFirst April 13, 2010; DOI:10.1158/1078-0432.CCR-09-2214

Cruz Biotechnology. Anti-TPX2 antibody was purchased from Novus Biologicals.

Formalin-fixed and paraffin-embedded liver tissues containing HCC were obtained from the National Cancer Center Hospital, and stained as described previously (15, 16). Immunoblot analysis of the KIM-1 cell lysate was done as described previously (15).

Animal experiments. Eight million KIM-1 cells suspended in 0.1 mL of PBS were s.c. inoculated into the flanks of 5-week-old female BALB/c nu/nu nude mice (SLC). Eight days later, the tumor-bearing mice were treated with siRNA together with atelocollagen (Koken Co., Ltd.), as described previously (17, 18). The final concentration of siRNA and atelocollagen was 11 μmol/L and 0.5%, respectively, and 200 μL of the siRNA solution were injected directly into each tumor. Tumor volume was determined every 3 days using the formula $V = 1/2\ (A \times B^2)$, where A and B represent the largest and smallest dimensions of the tumor, respectively.

Animal experiments were reviewed by the institutional ethics committee and performed in compliance with the

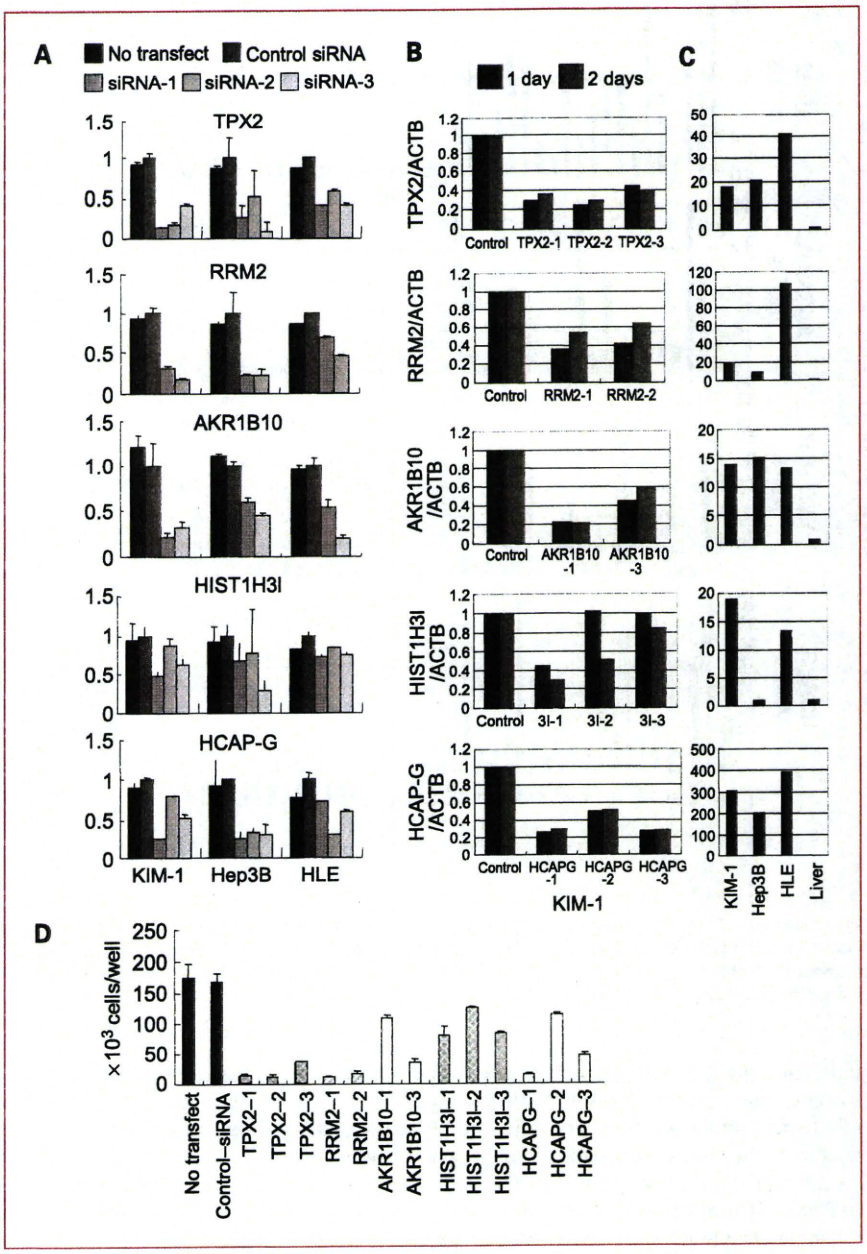

Fig. 2. siRNA-based functional screening. A, siRNA-mediated screening of genes required for proliferation of HCC cells. Three HCC cell lines (KIM-1, Hep3B, and HLE) were transfected with the indicated siRNAs, and the relative proportion of living cells was assessed 3 days later by measuring the mitochondrial succinate-tetrazolium reductase activity. Values for control siRNA were set at 1. B, reduction of the level of mRNA for each gene was determined by real-time PCR 1 and 2 days after transfection of KIM-1 cells with the indicated siRNAs. Values for control siRNA were set at 1. C, expression of each gene in HCC cell lines (KIM-1, Hep3B, and HLE) and normal liver tissue. D, confirmation of siRNA-mediated inhibition of HCC cell proliferation. KIM-1 cells were transfected with the indicated siRNAs, and the number of living cells was counted 3 days later by trypan blue dye exclusion using a hemocytometer.

Published OnlineFirst April 13, 2010; DOI:10.1158/1078-0432.CCR-09-2214

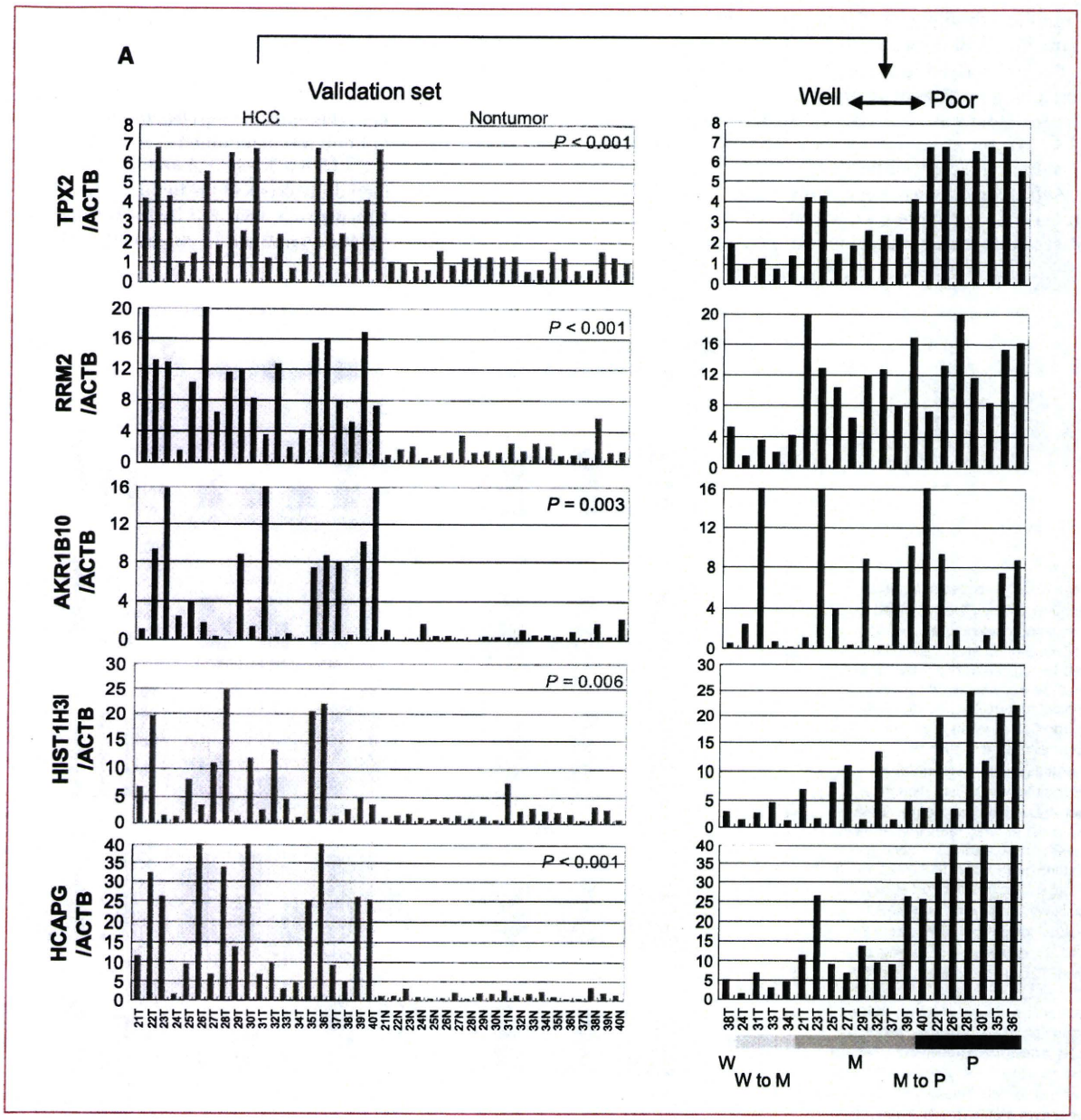

Fig. 3. Validation of differential expression. A, mRNA expression levels of selected genes in 20 independent pairs of HCC (21-40T) and adjacent nontumorous liver tissue (21-40N; validation set 1) determined by real-time PCR (left). The expression levels in HCC were realigned according to histologic differentiation (right). W, well differentiated; W to M, well to moderately differentiated; M, moderately differentiated; M to P, moderately to poorly differentiated, P, poorly differentiated.

guidelines for Laboratory Animal Research of the National Cancer Center Research Institute (Tokyo, Japan).

Statistical analysis. To extract differentially expressed genes from the array data, a paired *t* test with no correction was done (19) with asymptotic distribution to determine the *P* value. Correlations between array data and real-time PCR measurements were assessed using the Pearson correlation coefficient. The significance of differential gene expression between HCC and adjacent nontumorous liver tissue was assessed using the permutation paired *t* test followed by Bonferroni correction.

The weights and volumes of tumors are given as means (+SE). To evaluate the chronological effect of siRNAs on the growth of xenografts in comparison with control siRNA,

Published OnlineFirst April 13, 2010; DOI:10.1158/1078-0432.CCR-09-2214

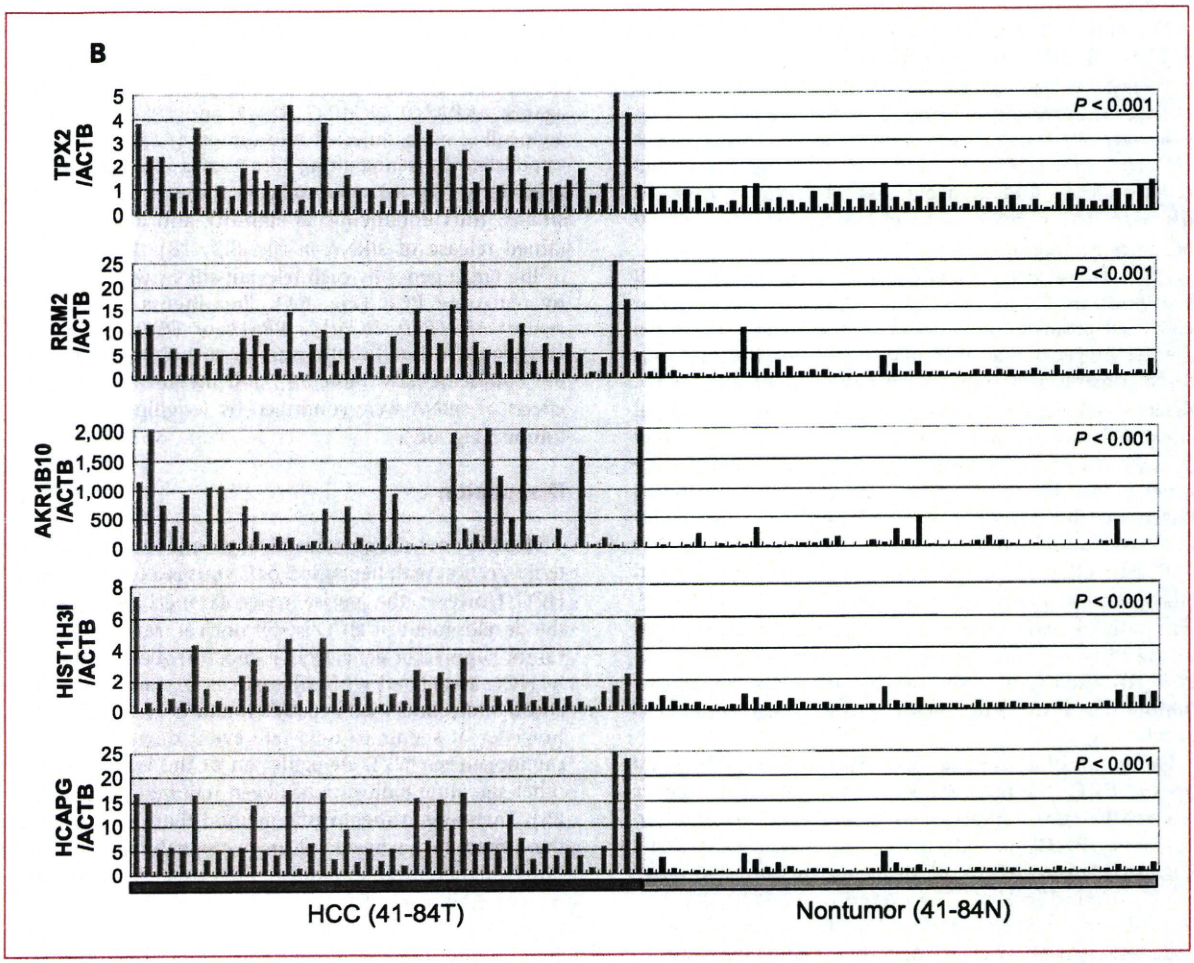

Fig. 3. *Continued.* B, expression levels of mRNAs for selected genes in 44 independent pairs of HCC (41-84T) and adjacent nontumorous liver tissue (41-84N; validation set 2) determined by real-time PCR.

a generalized linear mixed-effects model was used (20). The volume of the xenograft was modeled using γ-error distribution and log link function. This model considers each siRNA treatment as a fixed effect with control siRNA as an intercept and the number of days after implantation as a random effect. Estimates of variance components were obtained using the Laplacian approximation method, and the model fit was assessed using deviances. The significance of effects was estimated from the degree of freedom and t statistics followed by Bonferroni correction. Analysis was done using the lmer function for fitting generalized linear mixed-effects models, in the R statistical software package (version 2.6.0).

Results

Exon-based array analysis of HCC. Twenty paired samples of HCC and adjacent nontumorous liver tissue were subjected to genome-wide expression analysis using two different batches of the GeneChip Human Exon 1.0 ST arrays [discovery sets 1 (10 pairs) and 2 (10 pairs)]. Statistical analysis was done separately, and genes expressed differentially in the two sets were selected to eliminate any experimental bias caused by batch-to-batch variations. The exon array can detect mRNAs with low abundance as well as alternatively polyadenylated and spliced mRNA because the probes are designed to hybridize with the entire sequences of the transcripts (21). We identified 124 annotated genes that were differentially expressed between the background (nontumorous) liver tissue and HCC [at least a 3-fold change in transcription signal; $P < 0.001$ (paired t test with no correction)] in discovery set 1 (Supplementary Tables S2 and S3). The genes were clustered according to the similarity of their expression profiles (Fig. 1A), and the differential expression of representative genes was confirmed by real-time PCR (Fig. 1B). It was noteworthy that although 103 genes were found to be significantly downregulated, only 21 were apparently upregulated.

Published OnlineFirst April 13, 2010; DOI:10.1158/1078-0432.CCR-09-2214

We selected 9 genes (*AKR1B10*, *ANLN*, *CCNB1*, *HIST1H3B*, *HIST1H3C*, *HIST1H3I*, *RRM2*, *TOP2A*, and *TPX2*) whose expression was upregulated in HCC (≥3-fold change in transcription signal; $P < 0.001$, t test) in both discovery sets 1 and 2. Furthermore, two additional genes (*HCAP-G* and *DEPDC1*) were selected using a different criterion (>2.5-fold change across all of the 20 cases in discovery sets 1 and 2, and a raw signal of <50 in all 20 of the nontumorous liver tissues; $P < 0.05$, t test).

RNAi-based screening of genes required for HCC cell proliferation. To identify genes that are essential for HCC cell proliferation, siRNA-based screening was done for the 11 genes that were upregulated in HCC. Two or three constructs of siRNA were designed for each gene. Relative cell viability was evaluated by the mitochondrial succinate-tetrazolium reductase activity-based assay 3 days after transfection (Fig. 2A). We selected five genes (*TPX2*, *RRM2*, *HCAP-G*, *HIST1H3I*, and *AKR1B10*) based on the criterion that at least two siRNAs per gene reproducibly suppressed cell proliferation by >20% in all of three cell lines (KIM-1, Hep3B, and HLE). Representative data are shown in Fig. 2A and B. The baseline expression of these genes was determined in the three cell lines by real-time reverse transcription-PCR (RT-PCR; Fig. 2C). We confirmed the cell proliferation–inhibitory activity of the siRNA by counting the numbers of cells (Fig. 2D).

Validation of differential gene expression in additional cases of HCC. The increased expression of the five genes selected using the siRNA-based screen was validated in 20 cases of HCC (validation set 1) by real-time PCR (Fig. 3A). The expression of all five genes was confirmed to be increased in HCC. The expression of *TPX2*, *RRM2*, *HCAP-G*, and *HIST1H3* was associated with loss of histologic differentiation (Fig. 3A, right). The expression of *AKR1B10* was upregulated in HCC regardless of differentiation. We further confirmed the differential expression of these genes between HCC and nontumorous liver tissues in 44 additional independent cases of HCC (validation set 2) by real-time PCR (Fig. 3B).

In the 18 normal organs examined, no significant expression of *TPX2*, *RRM2*, or *HCAP-G* was observed, except for the thymus (Fig. 4, left), which is largely involuted in nonjuvenile adults. No organs showed higher expression of *AKR1B10* than was the case in HCC. We did not select *HIST1H3I*, as this gene showed high expression in several vital organs (Fig. 4).

Protein expression analysis. Expression of the products of four candidate genes, *TPX2*, *HCAP-G*, *RRM2*, and *AKR1B10*, was examined immunohistochemically in 19 independent cases of HCC (Fig. 5). In 84% (16 of 19) of the cases, AKR1B10 protein was detected in the cancer but was hardly evident in the adjacent nontumorous liver tissue. The nuclear staining of HCAP-G and TPX2 was stronger in HCC than in the adjacent nontumorous liver in 42% (8 of 19) and 58% (11 of 19) of cases, respectively. Patchy staining of RRM2 was observed in 84% (16 of 19) of the HCCs.

***Inhibition of tumor growth* in vivo.** Finally, we performed an *in vivo* experiment to evaluate the feasibility of the four selected genes as therapeutic targets. siRNA against *AKR1B10*, *HCAP-G*, *RRM2*, and *TPX2* mixed with atelocollagen was injected into tumors (31.5 ± 1.9 mm^3) established by xenografting KIM-1 cells into the flank of nude mice (Fig. 6). Atelocollagen forms a complex with siRNA, thus enhancing its stability and allowing sustained release of siRNA *in vivo* (17, 18). The silencing of the target genes by each relevant siRNA was confirmed by real-time PCR (Fig. 6A). Treatments with siRNA against *AKR1B10*, *HCAP-G*, *RRM2*, or *TPX2* given twice, 1 week apart, significantly suppressed tumor growth (Fig. 6B; Supplementary Table S6), and the growth-inhibitory effects of siRNA were confirmed by weighing the excised tumors (Fig. 6C).

Discussion

There is now strong epidemiologic evidence that persistent infection with hepatitis B or C virus is a major cause of HCC. However, the precise molecular mechanism behind the development of HCC is still unclear. Mutation in the tumor suppressor gene *TP53* is most frequently observed in HCC associated with aflatoxin B exposure as well as chronic infection with hepatitis B and C viruses (22–24); however, it seems to be a late event during multistep carcinogenesis (22). Deregulation of the Wnt as well as other signaling pathways has been reported in HCC (22, 25). Therefore, a therapeutic method that can normalize these aberrantly activated oncogenic signals would be clinically valuable. In an attempt to discover therapeutic targets with high specificity for HCC, we searched for genes that are specifically upregulated in HCC in comparison with nontumorous liver tissue and normal vital organs using high-density microarrays designed to detect all the exons in the human genome (Figs. 1 and 4). This was followed by siRNA-based screening of genes required for HCC cell proliferation (Fig. 2) as well as quantitative RT-PCR analysis and immunohistochemistry of additional cases (Figs. 3 and 5). We finally identified four candidate genes and confirmed their functional involvement in the tumor growth of HCC xenografts (Fig. 6). These genes, *AKR1B10*, *HCAP-G*, *RRM2*, and *TPX2*, were expressed strongly and specifically in HCC, which is highly dependent on these genes for proliferation, and their feasibility as therapy targets also seems to be supported by the literature.

RRM2 is a subunit of ribonucleotide reductase that catalyzes the conversion of ribonucleoside 5′-diphosphates into their corresponding 2′-deoxyribonucleotides. Because this reaction is the rate-limiting step of DNA synthesis, and inhibition of ribonucleotide reductase stops DNA synthesis and cell proliferation, RRM2 has been considered a promising target for cancer therapy (26).

TPX2 (C20ORF1) is a microtubule-associated protein whose expression is restricted to the S, G_2, and M phases of the cell cycle. Suppression of TPX2 expression by RNAi causes defects in microtubule organization during mitosis,

Published OnlineFirst April 13, 2010; DOI:10.1158/1078-0432.CCR-09-2214

leading to the formation of two microtubule asters that do not form a spindle (27). TPX2 is necessary for maintaining aurora A kinase in an active conformation (28, 29). Aurora kinases are essential for the regulation of chromosome segregation and cytokinesis during mitosis and have been reported to be overexpressed in a wide range of human tumors. Several aurora kinase inhibitors, such as VX-680/MK-0457, have been showed to have anticancer effects *in vitro* and *in vivo* (30, 31). The binding of TPX2 modulates the conformation of aurora A and reduces its affinity

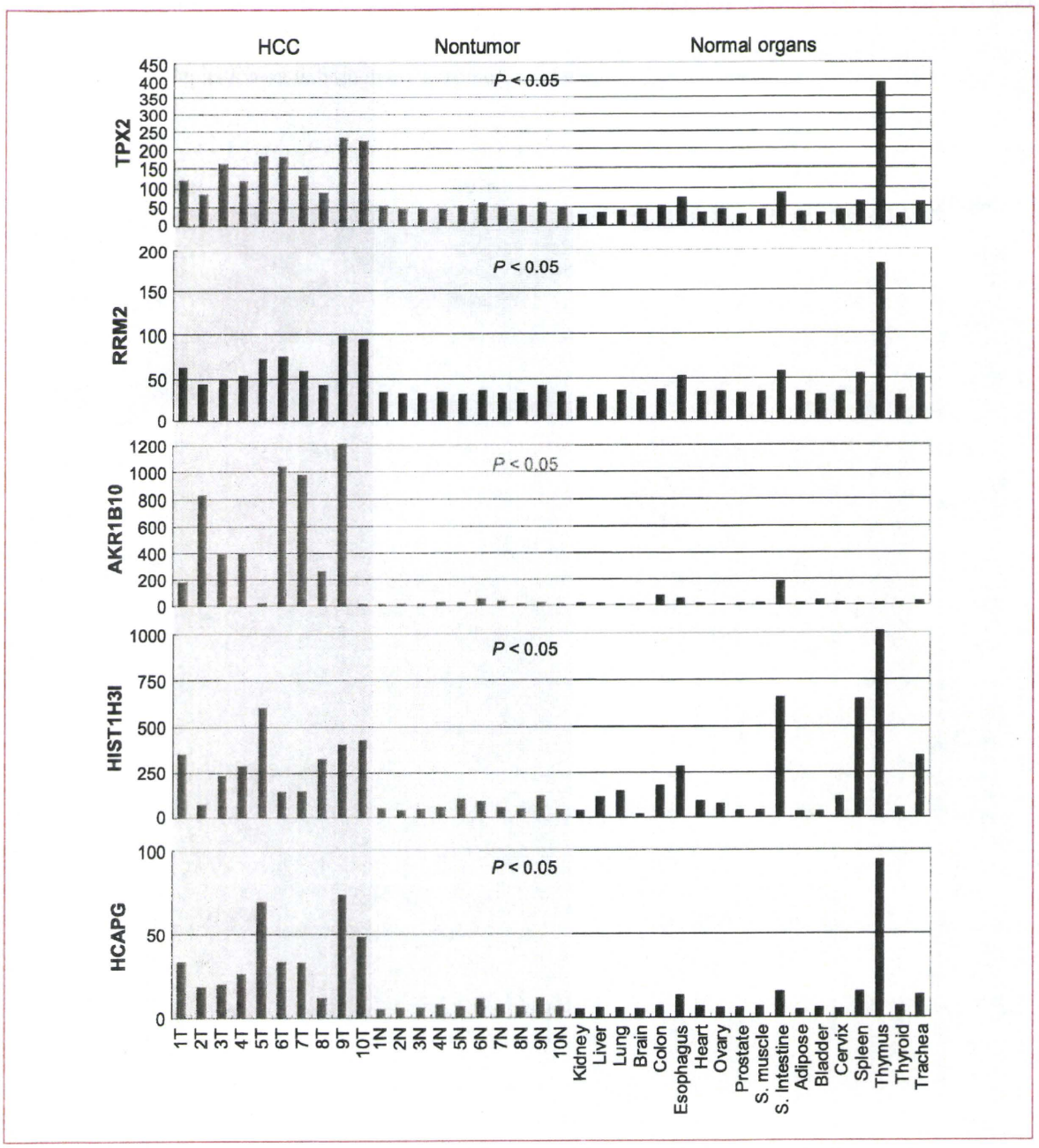

Fig. 4. Expression in normal organs. Expression levels of mRNAs for selected genes in 10 pairs of HCC (1-10T) and adjacent nontumorous liver tissue (1-10N; discovery set 1) and 18 normal organs determined by Human Exon 1.0 ST arrays (shown in arbitrary units). The significance of differential expression between HCC and adjacent nontumorous liver tissue was assessed using permutation paired *t* test, and Bonferroni-corrected *P* values are provided. S. muscle, skeletal muscle; S. intestine, small intestine.

Published OnlineFirst April 13, 2010; DOI:10.1158/1078-0432.CCR-09-2214

for VX-680 (32). Inhibition of TPX2 may increase the efficacy of this class of aurora kinase inhibitors.

HCAP-G is a component of the condensin complex that organizes the coiling topology of individual chromatids. Condensin also contributes to mitosis-specific chromosome compaction and is required for proper chromosome segregation, although the functional significance of HCAP-G in the condensing complex is largely unknown (33, 34).

AKR1B10 (ARL1, aldose reductase-like 1) was originally isolated as a new member of the aldo-keto reductase superfamily overexpressed in HCC and is reportedly related to the histologic differentiation of HCC (35, 36). AKR1B10 was also overexpressed in squamous cell carcinoma of the lung and its precursor conditions (37). Because the expression of AKR1B10 was highly specific to HCC and its inhibition suppressed tumor growth (Fig. 6), chemicals that specifically inhibit AKR1B10 activity may be useful anticancer drugs with minimal side effects.

It cannot be denied that many important genes were probably overlooked at every step of the present screen,

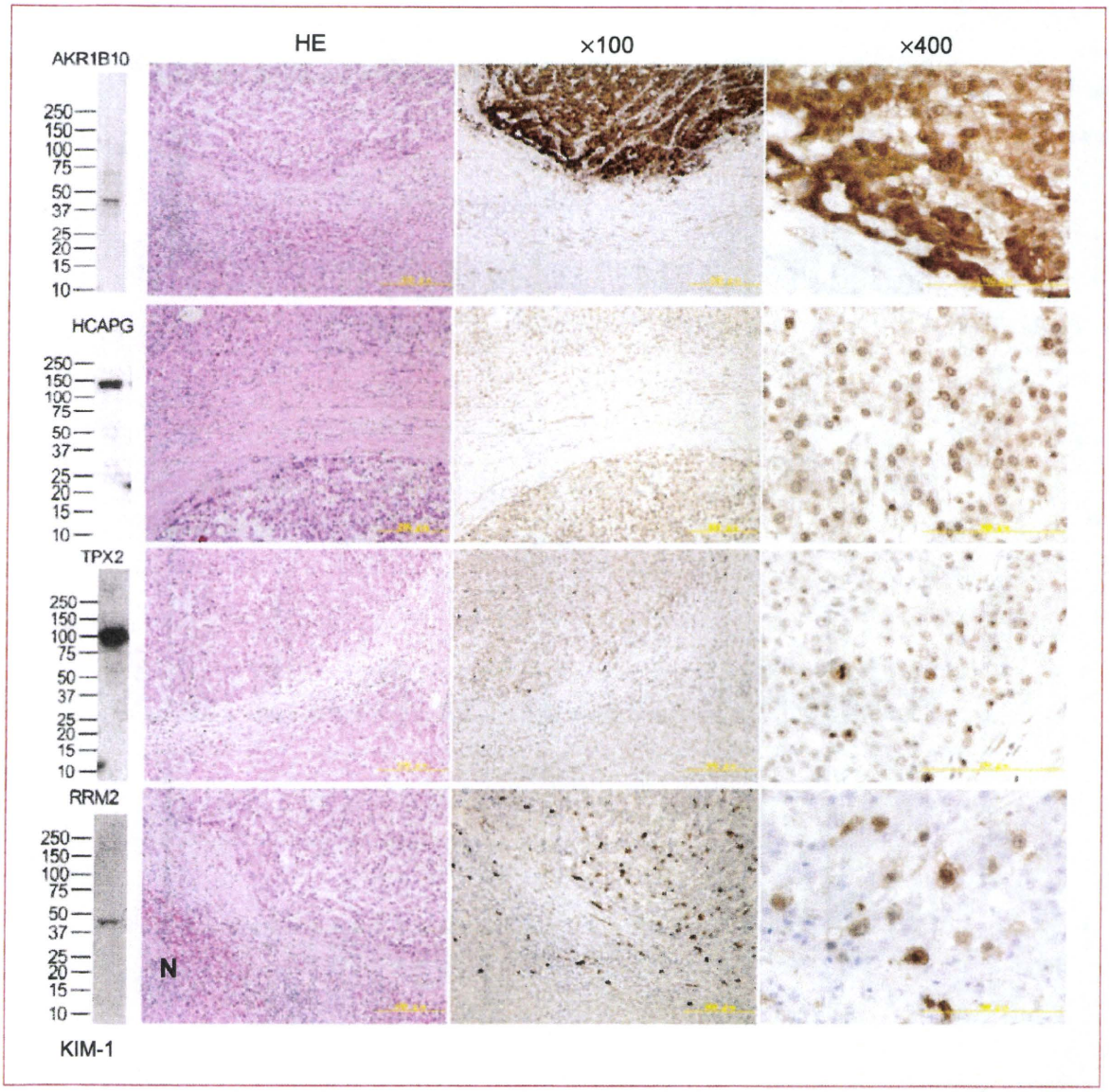

Fig. 5. Protein expression in HCC. Hematoxylin and eosin (HE) staining (original magnification, × 100) and immunoperoxidase staining (original magnifications, × 100 and × 400) of AKR1B10, HCAP-G, RRM2, and TPX2 proteins in HCC and adjacent nontumorous liver tissue. The specificity of antibodies was determined by immunoblotting of the KIM-1 cell lysate (left). N, nontumorous liver.

Published OnlineFirst April 13, 2010; DOI:10.1158/1078-0432.CCR-09-2214

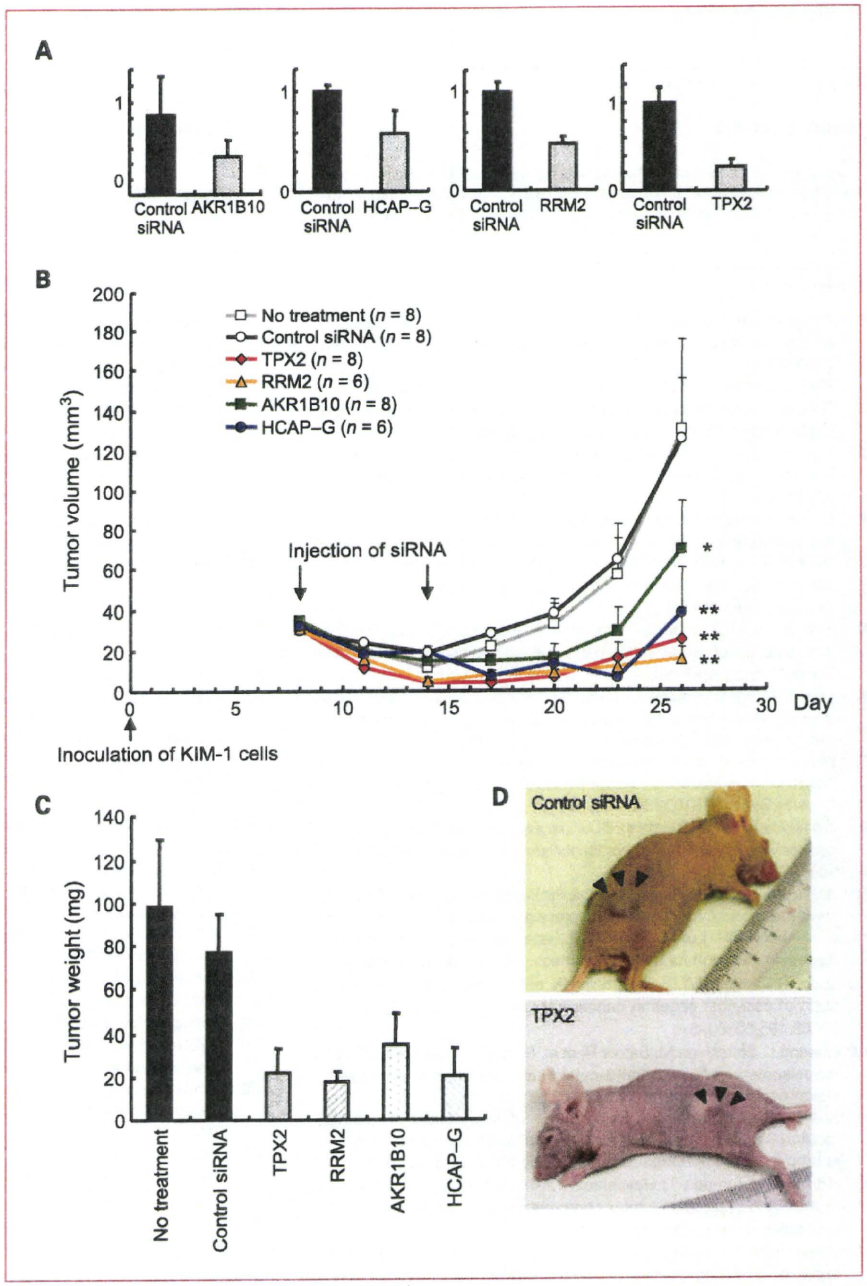

Fig. 6. Suppression of tumor growth by siRNA. A, KIM-1 cells were s.c. inoculated into the flanks of nude mice. Eight days later, control siRNA or siRNA against *AKR1B10, HCAP-G, RRM2*, or *TPX2* was injected into the developed tumors. The tumors were excised 2 days after the injection, and the expression levels of the indicated genes were determined by real-time PCR. Values of control siRNA were set at 1. B, chronological changes in tumor volume after two injections of the indicated siRNA. Volume of tumors was determined every 3 days as described in Materials and Methods. **, significantly different with a Bonferroni-corrected *P* value of <0.001. *, significantly different with a Bonferroni-corrected *P* value of 0.012. C, weight (mean + SE in mg) of xenografts measured 18 days after the second injection of the indicated siRNA and controls. D, macroscopic appearance of xenografts injected with control siRNA (top) and siRNA against TPX2 (bottom).

although the four selected genes seem to be highly relevant from a biological viewpoint. HCC has been recognized as a single category of disease; however, the overall gene expression patterns seem to differ markedly among individual cases. A search for the genes responsible for the different clinical outcomes of HCC will be the subject of a future study. We used the cell proliferation assay for siRNA-based functional screening. However, the use of other assays capable of evaluating cell motility, migration, drug sensitivity, or cell death may help to identify genes differing in their biological significance. The combination of genome-wide expression and functional screening described here provides a rapid and comprehensive approach that could be applicable for studies of various aspects of human cancer.

Disclosure of Potential Conflicts of Interest

No potential conflicts of interest were disclosed.

Published OnlineFirst April 13, 2010; DOI:10.1158/1078-0432.CCR-09-2214

Acknowledgments

We thank Dr. Masamichi Kojiro (Kurume University, Kurume, Japan) for providing the KIM-1 cells.

Grant Support

Program for Promotion of Fundamental Studies in Health Sciences conducted by the National Institute of Biomedical Innovation of Japan, the Third-Term Comprehensive Control Research for Cancer conducted by the Ministry of Health, Labor and Welfare of Japan, and generous grants from the Natio Foundation and the Princess Takamatsu Cancer Research Fund. These fund resources did not influence the study design or interpretation of the results.

The costs of publication of this article were defrayed in part by the payment of page charges. This article must therefore be hereby marked *advertisement* in accordance with 18 U.S.C. Section 1734 solely to indicate this fact.

Received 08/15/2009; revised 02/01/2010; accepted 03/08/2010; published OnlineFirst 04/13/2010.

References

1. El-Serag HB, Rudolph KL. Hepatocellular carcinoma: epidemiology and molecular carcinogenesis. Gastroenterology 2007;132:2557–76.
2. Hernandez-Boluda JC, Cervantes F. Imatinib mesylate (Gleevec, Glivec):a new therapy for chronic myeloid leukemia and other malignancies. Drugs Today (Barc) 2002;38:601–13.
3. Fong T, Morgensztern D, Govindan R. EGFR inhibitors as first-line therapy in advanced non-small cell lung cancer. J Thorac Oncol 2008;3:303–10.
4. Llovet JM, Ricci S, Mazzaferro V, et al. Sorafenib in advanced hepatocellular carcinoma. N Engl J Med 2008;359:378–90.
5. Di Maio M, Daniele B, Perrone F. Targeted therapies: role of sorafenib in HCC patients with compromised liver function. Nat Rev Clin Oncol 2009;6:505–6.
6. Hideshima T, Chauhan D, Richardson P, Anderson KC. Identification and validation of novel therapeutic targets for multiple myeloma. J Clin Oncol 2005;23:6345–50.
7. Izzo F, Marra P, Beneduce G, et al. Pegylated arginine deiminase treatment of patients with unresectable hepatocellular carcinoma: results from phase I/II studies. J Clin Oncol 2004;22:1815–22.
8. Drew Y, Plummer R. The emerging potential of poly(ADP-ribose) polymerase inhibitors in the treatment of breast cancer. Curr Opin Obstet Gynecol 2010;22:67–71.
9. Whitehurst AW, Bodemann BO, Cardenas J, et al. Synthetic lethal screen identification of chemosensitizer loci in cancer cells. Nature 2007;446:815–9.
10. Silva JM, Marran K, Parker JS, et al. Profiling essential genes in human mammary cells by multiplex RNAi screening. Science 2008;319:617–20.
11. Schlabach MR, Luo J, Solimini NL, et al. Cancer proliferation gene discovery through functional genomics. Science 2008;319:620–4.
12. Luo B, Cheung HW, Subramanian A, et al. Highly parallel identification of essential genes in cancer cells. Proc Natl Acad Sci U S A 2008;105:20380–5.
13. Huang L, Shitashige M, Satow R, et al. Functional interaction of DNA topoisomerase IIα with the β-catenin and T-cell factor-4 complex. Gastroenterology 2007;133:1569–78.
14. Shitashige M, Naishiro Y, Idogawa M, et al. Involvement of splicing factor-1 in β-catenin/T-cell factor-4-mediated gene transactivation and pre-mRNA splicing. Gastroenterology 2007;132:1039–54.
15. Honda K, Yamada T, Hayashida Y, et al. Actinin-4 increases cell motility and promotes lymph node metastasis of colorectal cancer. Gastroenterology 2005;128:51–62.
16. Yamaguchi U, Nakayama R, Honda K, et al. Distinct gene expression-defined classes of gastrointestinal stromal tumor. J Clin Oncol 2008;26:4100–8.
17. Minakuchi Y, Takeshita F, Kosaka N, et al. Atelocollagen-mediated synthetic small interfering RNA delivery for effective gene silencing *in vitro* and *in vivo*. Nucleic Acids Res 2004;32:e109.
18. Takeshita F, Minakuchi Y, Nagahara S, et al. Efficient delivery of small interfering RNA to bone-metastatic tumors by using atelocollagen *in vivo*. Proc Natl Acad Sci U S A 2005;102:12177–82.
19. Shi L, Reid LH, Jones WD, et al. The MicroArray Quality Control (MAQC) project shows inter- and intraplatform reproducibility of gene expression measurements. Nat Biotechnol 2006;24:1151–61.
20. Bolker BM, Brooks ME, Clark CJ, et al. Generalized linear mixed models: a practical guide for ecology and evolution. Trends Ecol Evol 2009;24:127–35.
21. Gardina PJ, Clark TA, Shimada B, et al. Alternative splicing and differential gene expression in colon cancer detected by a whole genome exon array. BMC Genomics 2006;7:325.
22. Hussain SP, Schwank J, Staib F, Wang XW, Harris CC. TP53 mutations and hepatocellular carcinoma: insights into the etiology and pathogenesis of liver cancer. Oncogene 2007;26:2166–76.
23. Gouas D, Shi H, Hainaut P. The aflatoxin-induced TP53 mutation at codon 249 (R249S): biomarker of exposure, early detection and target for therapy. Cancer Lett 2009;286:29–37.
24. Villanueva A, Newell P, Chiang DY, Friedman SL, Llovet JM. Genomics and signaling pathways in hepatocellular carcinoma. Semin Liver Dis 2007;27:55–76.
25. Katoh H, Shibata T, Kokubu A, et al. Genetic inactivation of the APC gene contributes to the malignant progression of sporadic hepatocellular carcinoma: a case report. Genes Chromosomes Cancer 2006;45:1050–7.
26. Shao J, Zhou B, Chu B, Yen Y. Ribonucleotide reductase inhibitors and future drug design. Curr Cancer Drug Targets 2006;6:409–31.
27. Gruss OJ, Vernos I. The mechanism of spindle assembly: functions of Ran and its target TPX2. J Cell Biol 2004;166:949–55.
28. Bayliss R, Sardon T, Ebert J, Lindner D, Vernos I, Conti E. Determinants for Aurora-A activation and Aurora-B discrimination by TPX2. Cell Cycle 2004;3:404–7.
29. Marumoto T, Zhang D, Saya H. Aurora-A—a guardian of poles. Nat Rev Cancer 2005;5:42–50.
30. Keen N, Taylor S. Aurora-kinase inhibitors as anticancer agents. Nat Rev Cancer 2004;4:927–36.
31. Harrington EA, Bebbington D, Moore J, et al. VX-680, a potent and selective small-molecule inhibitor of the Aurora kinases, suppresses tumor growth *in vivo*. Nat Med 2004;10:262–7.
32. Anderson K, Yang J, Koretke K, et al. Binding of TPX2 to Aurora A alters substrate and inhibitor interactions. Biochemistry 2007;46:10287–95.
33. Gerlich D, Hirota T, Koch B, Peters JM, Ellenberg J. Condensin I stabilizes chromosomes mechanically through a dynamic interaction in live cells. Curr Biol 2006;16:333–44.
34. Lam WW, Peterson EA, Yeung M, Lavoie BD. Condensin is required for chromosome arm cohesion during mitosis. Genes Dev 2006;20:2973–84.
35. Scuric Z, Stain SC, Anderson WF, Hwang JJ. New member of aldose reductase family proteins overexpressed in human hepatocellular carcinoma. Hepatology 1998;27:943–50.
36. Teramoto R, Minagawa H, Honda M, et al. Protein expression profile characteristic to hepatocellular carcinoma revealed by 2D-DIGE with supervised learning. Biochim Biophys Acta 2008;1784:764–72.
37. Li CP, Goto A, Watanabe A, et al. AKR1B10 in usual interstitial pneumonia: expression in squamous metaplasia in association with smoking and lung cancer. Pathol Res Pract 2008;204:295–304.

Generation of genetically modified rats from embryonic stem cells

Masaki Kawamata and Takahiro Ochiya[1]

Section for Studies on Metastasis, National Cancer Center Research Institute, 1-1 Tsukiji, 5-chome, Chuo-ku, Tokyo 104-0045, Japan

Communicated by Takashi Sugimura, National Cancer Center, Tokyo, Japan, June 30, 2010 (received for review April 22, 2010)

At present, genetically modified rats have not been generated from ES cells because stable ES cells and a suitable injection method are not available. To monitor the pluripotency of rat ES cells, we generated *Oct4*-Venus transgenic (Tg) rats via a conventional method, in which Venus is expressed by the *Oct4* promoter/enhancer. This monitoring system enabled us to define a significant condition of culture to establish authentic rat ES cells based on a combination of 20% FBS and cell signaling inhibitors for Rho-associated kinase, mitogen-activated protein kinase, TGF-β, and glycogen synthase kinase-3. The rat ES cells expressed ES cell markers such as *Oct4*, *Nanog*, *Sox2*, and *Rex1* and retained a normal karyotype. Embryoid bodies and teratomas were also produced from the rat ES cells. All six ES cell lines derived from three different rat strains successfully achieved germline transmission, which strongly depended on the presence of the inhibitors during the injection process. Most importantly, high-quality Tg rats possessing a correct transgene expression pattern were successfully generated via the selection of gene-manipulated ES cell clones through germline transmission. Our rat ES cells should be sufficiently able to receive gene targeting as well as Tg manipulation, thus providing valuable animal models for the study of human diseases.

genetic engineering | rat | embryonic stem cells

The laboratory rat was the earliest mammalian species domesticated for scientific research and has been used as an animal model in physiology, toxicology, nutrition, behavior, immunology, and neoplasia for over 150 y (1). Despite this history, rats lag far behind mice in functional genetic studies and the generation of knockout animal models reflecting human diseases because of the absence of germline-competent rat ES cells, which are vital in a reverse genetics approach (2, 3). Recently, gene-targeting rats were created by the zinc finger nuclease strategy (4). However, the system is not available for most researchers because a special technique is required to make algorithm-based sequence-specific DNA nucleases. Thus, establishment of rat ES cells has been desired to produce gene-targeting rats, such as mutant mice, routinely.

Although we established rat ES cell lines with chimeric contribution, none could complete germline transmission (5). Soon after our report, other groups succeeded in establishing rat ES cells with germline transmission by using 2i, mitogen-activated protein kinase (MEK) inhibitor PD0325901, and glycogen synthase kinase-3 (GSK3) inhibitor CHIR99021 (6, 7). The 2i is widely used in the establishment of ES cells or induced pluripotent stem (iPS) cells in mice (8, 9), rats (6, 7, 10), and humans (10). Thus, the inhibition of MEK and GSK3 has been thought to maintain a ground state of pluripotency in various species. Rat iPS cells with chimeric contribution were established by using an inhibitor of type 1 TGF-β receptor Alk5 (A-83-01) with the 2i, although germline transmission was not accomplished (10). Furthermore, a combination of MEK and ALK5 inhibitors dramatically improved the efficiency of iPS cell generation from human fibroblasts (11). These reports indicate that the inhibition of TGF-β signaling also plays a key role in pluripotency.

It is known that rat ES cells present critical problems in that undifferentiated cells cannot proliferate from single cells after enzymatic dissociation (5) and that chromosomal instability is caused by long-term culture, resulting in the failure of germline transmission (5–7). Recently, Watanabe et al. found that a Rho-associated kinase inhibitor Y-27632 (12) blocks apoptosis and enhances the proliferation of human ES cells after their dissociation into single cells by enzymatic treatment (13). The propagated ES cells cultured by Y-27632 were positive for alkaline phosphatase (ALP) and marker genes such as E-cadherin, Oct4, and SSEA4, and the number of chromosomes was normally maintained during long-term culture (13). These recent reports indicate the suitability of cell signaling inhibitors in the establishment of rat ES cells.

To generate genetically modified rats, highly potent ES cells that can stably contribute to germline chimeras have to be established. As a first step, we generated *Oct4*-Venus transgenic (Tg) rats, in which Venus [YFP mutant (14)] is expressed by the *Oct4* promoter/enhancer. This Tg line enables us to monitor the pluripotency of rat ES cells during the process of establishment. We addressed suitable combinations of the signaling inhibitors based on a culture medium that included 20% FBS. As a result, the use of a combination of four inhibitors, Y-27632, PD0325901, A-83-01, and CHIR99021 (termed YPAC), allowed the establishment of authentic rat ES cells and appeared necessary in the blastocyst injection process for the generation of germline chimeras. Finally, we report that high-quality Tg rats retaining reproductive ability can be generated from rat ES cells.

Results

YPAC Maintains Pluripotency in the Outgrowths of *Oct4*-Venus Tg Blastocysts. We first generated a Tg rat carrying an *Oct4*-Venus fluorescence reporter to monitor pluripotency during establishment of rat ES cells and to investigate development of the ES cells into germ cells in fetal gonads of chimeras. The 3.9-kb *Oct4* (also known as *Pou5f1*) promoter includes both the proximal enhancer and distal enhancer, which gives *Oct4* expression in morula, inner cell mass (ICM), epiblast, primordial germ cells (PGCs), and ES cells (15). In the Tg embryo, Venus was detected specifically in PGCs in the gonad (Fig. S1). This result corresponds to previous reports regarding *Oct4*-reporter Tg mice (16).

Outgrowths were examined from the Tg blastocysts in a basic medium containing 20% FBS, which is generally used for mouse ES cell culture, with or without YPAC. In its absence, Venus fluorescence was decreased at day 3 after plating and disappeared at day 7 despite the fact that ES-like cells propagated and formed a domed structure similar to the mouse ES cell colony (Fig. 1*A*). In the presence of YPAC, ICM cells rapidly propagated while maintaining Venus fluorescence even at day 7. The fluorescence was not observed in differentiated cells (Fig. 1*B*). The expression levels of ES cell marker genes *Oct4*, *Nanog*, *Sox2*, and *Rex1* in ICM cells with YPAC were higher than those without YPAC (Fig. 1*C*).

Author contributions: M.K. and T.O. designed research; M.K. performed research; M.K. analyzed data; and M.K. and T.O. wrote the paper.

The authors declare no conflict of interest.

Freely available online through the PNAS open access option.

[1]To whom correspondence should be addressed. E-mail: tochiya@ncc.go.jp.

This article contains supporting information online at www.pnas.org/lookup/suppl/doi:10.1073/pnas.1009582107/-/DCSupplemental.

DEVELOPMENTAL BIOLOGY

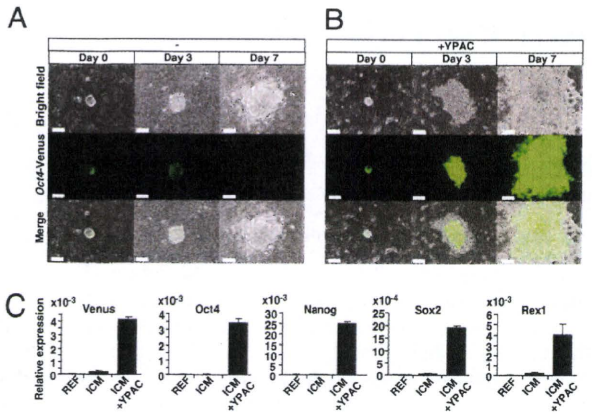

Fig. 1. Outgrowth of ICM cells in YPAC medium. Outgrowth of blastocysts in −YPAC (*A*) or +YPAC (*B*) medium. E4.5 blastocysts were plated onto mitotically inactivated MEFs. (*C*) qPCR analysis of Venus, *Oct4*, *Nanog*, *Sox2*, and *Rex1* in ICM cells. Seven days after plating, RNAs were extracted from domed segments of ICM cells derived from seven or four blastocysts in −YPAC or +YPAC medium, respectively. Transcript levels were normalized to *Gapdh* levels. Data are the mean ± SD of one biological sample assayed in three independent experiments and represent relative expression levels of indicated genes in REFs, ICM (−YPAC), and ICM (+YPAC). (Scale bars: 100 μm.)

In its absence, the decrease of *Oct4* mRNA was parallel to that of Venus mRNA and fluorescence. In the YPAC condition, blastocyst outgrowth was observed in 51 samples for all the tested embryos regardless of the strains (Table 1). The blastocyst strains were derived from a hybrid of Tg Wistar and wild-type Wistar (TgWW, albino), wild-type Wistar (WW, albino), Long–Evans agouti [LEA (LL, agouti)], or a hybrid of Tg Wistar and LEA (TgWL, agouti).

Small Molecules Enable Efficient Derivation and Maintenance of Rat ES Cells. The outgrowths were dissociated into small pieces and replated in the same mouse embryonic fibroblasts (MEFs)/YPAC condition. After undifferentiated colonies appeared, they were split into single cells by Accutase (Innovative Cell Technologies, Inc.). These cells attached on the MEFs and formed domed colonies, which can be passaged continuously (Fig. 2*A Upper Left*). Although most of the ES cells showed ALP activity (Fig. 2*B Left*) and Oct4 protein expression (Fig. 2*D Left*) even after long passages, Venus fluorescence became weak or negative (Fig. 2*A Lower Left*). The expression pattern of Venus mRNA was not parallel to that of *Oct4* between TgWL1 and TgWW1 cell lines (Fig. 2*C*). These results suggest that the function of the *Oct4*-Venus transgene is unavailable in rat ES cell lines. The long-passaged rat ES cells might receive epigenetic silencing effects.

The ES cell lines maintained higher mRNA levels of ES cell marker genes *Oct4*, *Sox2*, *Nanog*, and *Rex1* compared with rat embryonic fibroblasts (REFs) (Fig. 2*C*). Microarray analyses also indicated that global gene expression was remarkably different between ES cells and REFs but similar between the three ES cell lines TgWL1, TgWW1, and LL1 (Fig. S2). Nanog and Sox2 proteins were also detected in ES cells (Fig. 2*D*). The karyotypes of 50 cells were analyzed by G-band staining. Most of the cells exhibited a normal chromosomal number of 42 in TgWL1 (70%, XX, P14), TgWL2 (84%, XX, P7; Fig. 2*E*), TgWW1 (92%, XX, P5), and LL1 (84%, XX, P6). TgWW1 cells (2.6×10^6) could form a teratoma 34 d after transplantation under the skin of an immunodeficient SCID mouse. A histological examination showed that the tumor contained all three germ layers, including the intestinal epithelium (endoderm), cartilage (mesoderm), and neuronal rosette (ectoderm) (Fig. 2*F*).

Table 1. Establishment of rat ES cells from blastocysts in YPAC medium

Strain	No. ICMs	Outgrowth†	Continue	Cell line‡
TgWL	2	2	2	2
TgWW	15	15	1	1
WW	9	9	1	1
LL	19	19	2	2
TgWW*	3	3	2	2
WW*	3	3	0	0
Total	51	51 (100%)	8	8 (100%)

*Specific serum was used (FBS for MEF culture; EQUITECH-BIO, Inc.).
†Outgrowth refers to the expansion of the ICM.
‡Cell line refers to continuous culture of at least seven passages. Single-cell passage was begun at passages 1–3. Domed colonies with undifferentiated cells are continuously formed from single cells.

To confirm the effect of Y, the rat ES cells were cultured in a PAC medium. Under this condition, sparse colonies appeared because of a failure in the adherence process of single cells on MEFs, although the colonies kept undifferentiated morphology and ALP activity (Fig. 2*A Middle* and *B Middle*). Although only Y enabled most of the single cells to adhere on MEFs and to proliferate, they were differentiated and did not show ALP activity (Fig. 2 *A Right* and *B Right*).

The classic method to induce ES cell differentiation is to allow the cells to grow in suspension and to form 3D aggregates known as embryoid bodies (EBs) (17). Dissociated ES cells were plated into low-cell-binding dishes in the basal medium. EBs could be formed from the ES cells at a much lower efficiency compared with their formation from mouse ES cells (Fig. 2*E*). The expression of marker genes was decreased during the process of EB differentiation (Fig. 2*I*). In the presence of PAC, cells aggregated with high efficiency and formed a clear 3D structure (Fig. 2*F*). The EBs with PAC at day 7 still sustained high expression levels of the marker genes (Fig. 2*I*). These results suggest that PAC enables ES cells to maintain pluripotency, whereas for rat ES cells to adhere on MEFs, Y is necessary.

YPAC Injection Engenders Germline Chimeras. First, we produced stable transfectant ES cells expressing cyan fluorescence from a CAG-AmCyan1 transgene to monitor cell fate in the blastocyst after injection or chimerism in fetuses (Fig. 3*A*). Before generation of the chimera, the potential of YPAC was investigated during the injection and blastocyst incubation processes because the rat ES cells tended to differentiate easily in the absence of inhibitors (Fig. 2 *A*, *B*, and *E*). There was no difference between normal and YPAC injection 5 h after incubation; in both cases, several cyan-positive cells adhered on the ICM and trophectoderm. However, 30 h after incubation, few cyan-positive cells existed in the blastocysts in the absence of YPAC, whereas in its presence, several cells remained on the ICM surface. Furthermore, blastocyst shape was maintained by the addition of YPAC even after incubation for 30 h (Fig. 3*B*). This result suggests that administration of YPAC during the injection process causes both ES cells and recipient blastocysts to block differentiation or apoptosis. This YPAC injection method enabled generation of chimeric embryos showing positivity for cyan but negativity for Venus in the surface of skin and kidney. Venus-positive cells were detected specifically in the gonads, showing the successful development of the ES cells into germ cells (Fig. 3*C*). We also succeeded in generating germline chimeras using all other cell lines by detecting Venus fluorescence in the fetal gonad (Table 2). The germline chimeras were detected in 2 of 12 fetuses by using long-cultured TgWL2 cells at passage 22 (Table 2 and Fig. S3).

To investigate the pluripotent ability of ES cells, we carried out a single-cell injection into a blastocyst. After injection of the

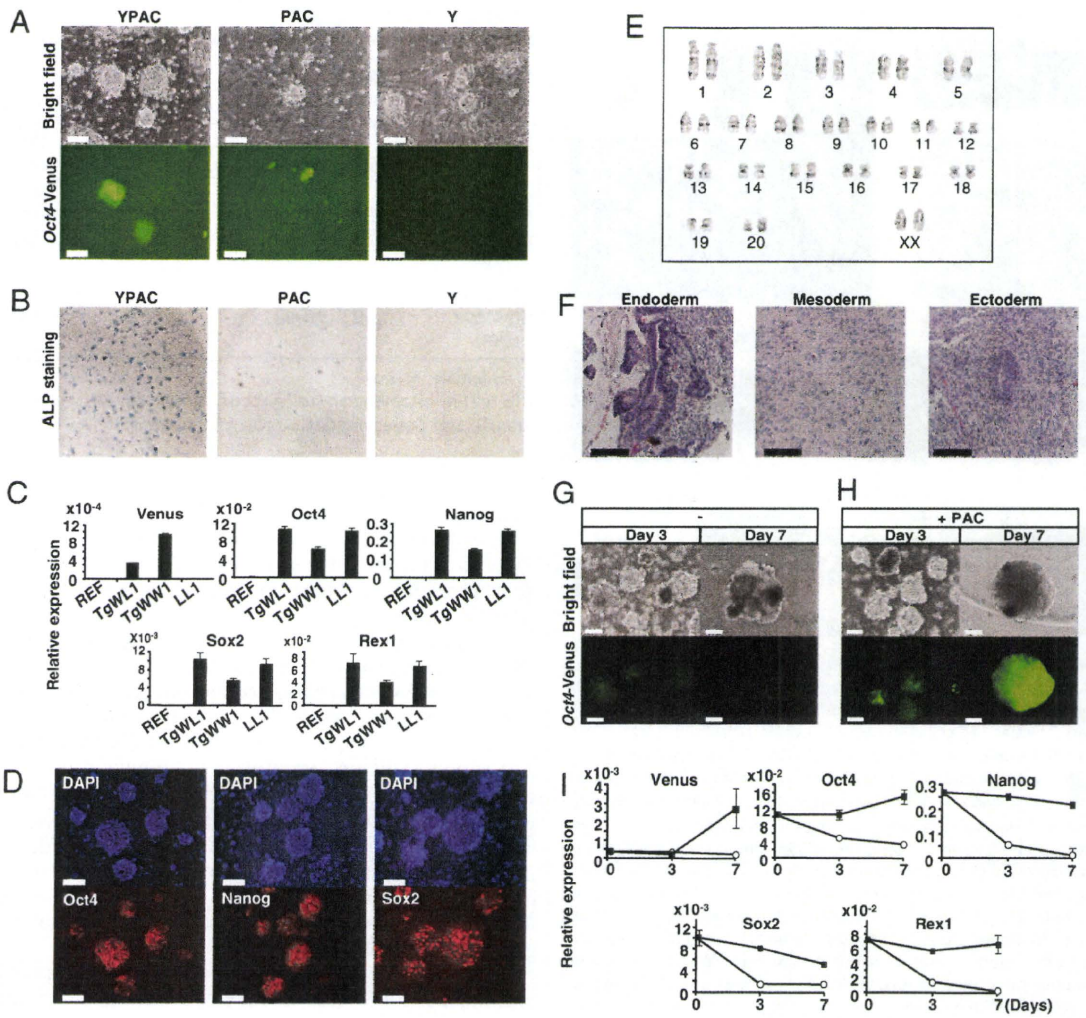

Fig. 2. Characterization of rat ES cells. Effect of Y-27632 (*A*) and ALP (*B*) staining. Dissociated single cells (1×10^5 TgWW1, passage 6) were plated into a well of six-well plates under the condition of MEFs with YPAC (*Left*), PCA (*Center*), or Y (*Right*). (*B*) ALP staining in these cells. (*C*) qPCR analysis of Venus, *Oct4*, *Nanog*, *Sox2*, and *Rex1* in rat ES cell lines. Transcript levels were normalized to *Gapdh* levels. Data are the mean ± SD of one biological sample assayed in three independent experiments and represent the relative expression levels of indicated genes in REF, TgWL1, TgWW1, and LL1. (*D*) Immunofluorescence staining for *Oct4*, *Nanog*, and *Sox2* in rat ES cells. (*E*) Cytogenetic analysis in rat ES cells by G-band staining. Representative data of TgWL2 at passage 7 indicate a chromosomal number of 42, including an XX gender chromosome. (*F*) Histological sections of a teratoma derived from a TgWW1 ES cell line showing three germ layers. Embryoid bodies (TgWL1) were produced in a basic ES cell medium with (*H*) or without (*G*) three PAC inhibitors, excluding Y-27632. A time-course experiment was performed, and the EBs were observed at days 3 and 7. (*I*) qPCR analysis of Venus, *Oct4*, *Nanog*, *Sox2*, and *Rex1* in EBs. Transcript levels were normalized to *Gapdh* levels. Data are the mean ± SD of one biological sample assayed in three independent experiments and represent the relative expression levels of indicated genes in EBs produced without inhibitors (○) or with PAC (■) at days 0, 3, and 7. (Scale bars: 100 μm.)

TgWW1 cell at passage 9, the single cell attached to the internal surface of the blastocyst (Fig. 3*D*). In an embryo day (E) 16.0 fetus gonad, germ cell differentiation was confirmed by the detection of Venus fluorescence (Fig. 3*E*).

To generate coat-color chimeras, TgWL1 cells were injected into Wistar blastocysts using the YPAC injection method. Eight of 23 coat-color chimeras were obtained from the TgWL1 cell line at passage 11 or 12 (Fig. 3*F Right* and Table 3). Without the YPAC injection method, a coat-color chimera was hardly generated despite the fact that the same cell line, TgWL1, was used at earlier passages 6–8 (Fig. 3*F Left* and Table 3). Only 1 male chimera of 44 pups was obtained, but the chimerism was very sparse (Fig. S4). The generation of coat-color chimeras was successful in all six cell lines (Table 3). Those from cell line TgWW1 or LL1 are shown in Fig. S5. After mating with male rats, germline transmission was accomplished in adult female chimeras derived from all six cell lines independent of rat strains (Fig. 3*G* and Table 3). Genotyping analysis indicated that the *Oct4*-Venus transgene of the ES cells (TgWL2) was transmitted to filial (F)1 germline offspring with an agouti coat color (Fig. 3*H*).

Generation of ES Cell-Derived Tg Rats. We proposed to generate ES cell-derived transgenic (esTg) rats harboring the *Oct4*-Venus transgene, which shows a correct Venus expression pattern similar to Oct4 protein (Fig. 2*D*). After introduction of the *Oct4*-Venus transgene containing the same *Oct4* promoter/enhancer region as used in the generation of the conventional transgenic (cvTg) rats, 15 Venus-positive colonies (LL2 line) were picked up. After two passages, silencing of Venus gene expression occurred in 13 of 15 clones, resulting in an apparent heterogeneity in the fluorescence of Venus-positive clones (Fig. 4*A*, arrowheads), whereas only 2 clones kept homogenous Venus fluorescence (Fig. 4*B*). Chimeric

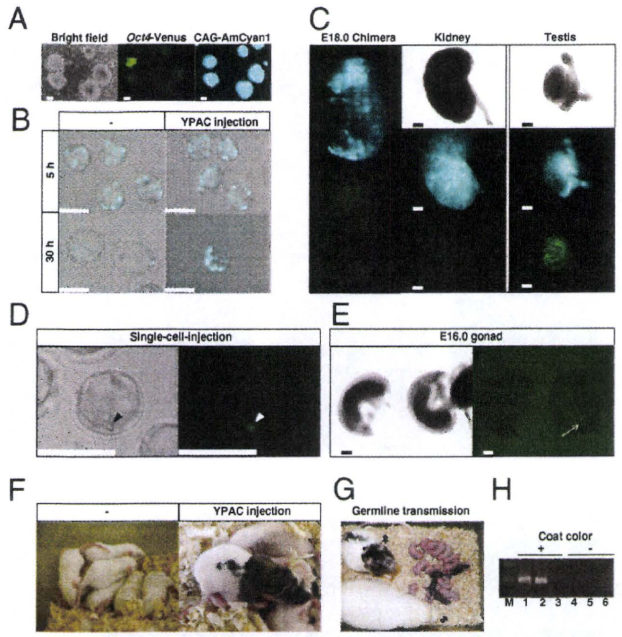

Fig. 3. Generation of germline chimeras by YPAC injection method. (*A*) Expression of AmCyan1 in stable transfectant clones (TgWW1 + C) generated by nucleofection with CAG-AmCyan1 plasmids. (*B*) Effect of YPAC during injection process. The basic ES cell medium with (*Right*) or without (*Left*) YPAC was used during the processes: injection of TgWW1 + C cells into blastocysts and incubation of the blastocysts for 30 h. (*C*) Generation of germline chimeras in embryos. TgWW1 + C cells were injected into Wistar blastocysts. Venus or AmCyan1 fluorescence was observed in E18.0 whole embryo, kidney, and testis. (*D* and *E*) Generation of germline chimeras by single-cell injection. (*D*) A single cell (TgWW1) was injected into a blastocyst. The image shows the injected blastocyst 3 h after incubation. The arrowhead indicates the injected single cell. (*E*) Venus-positive germ cells were detected in gonad at E16.0 (arrow). (*F*) Generation of coat-color chimeras by the YPAC injection. (*G*) Germline transmission in adult chimeras. The chimera (TgWL1) was mated with a Wistar male rat. Germline pups (4 of 16) were confirmed by an agouti coat color. (*H*) Genotyping analysis of F1 offspring of female chimera (TgWL2). The Venus region was amplified by PCR from genomic DNA of tail. M, 100-bp DNA marker; 1, 2, and 3, germline offspring with an agouti coat color; 4, 5, and 6, coat color-negative (albino) offspring. (Scale bars, *A*, *B*, and *D*: 100 μm; *C* and *E*: 300 μm.)

rats were produced via injection of the stable clone into Wistar blastocysts. Furthermore, germline transmission with the *Oct4*-Venus transgene was accomplished in the female chimeras (Fig. 4*C* and Table 3). The esTg embryos at 16.0 days postcoitum (dpc) exhibited Venus fluorescence in the gonads (Fig. 4*D*). The esTg rats were able to mature to adults without apparent abnormalities and had normal reproductive ability. We established ES cell lines from esTg blastocysts to confirm an expression pattern of Venus fluorescence. During outgrowth, their Venus expression pattern (Fig. 4*E*) was similar to that of cvTg blastocysts (Fig. 1*B*). However, long-passaged esTg cell lines ($n = 3$) maintained stable Venus expression in the ES cells (Fig. 4*F*). This result indicates our success in generating high-quality esTg rats possessing a correct expression pattern of Venus under the *Oct4* promoter/enhancer.

Discussion

Our results demonstrated that the use of a combination of serum and cell signaling inhibitors during outgrowth, cell culture, and blastocyst injection leads to the generation of germline chimeras with extremely high efficiency. Furthermore, we generated genetically modified rats from ES cells, termed esTg rats, growing up healthily and retaining reproductive ability. The advantage of this technology of using rat ES cells is that we can select Tg ES

Table 2. Summary of germline chimeras: Germ cell development in fetal gonad judged by Venus fluorescence

Cell line (gender)	Passage no.	Host blastocyst	Injected embryos	Fetal no.	Germline chimera
TgWL2 (XX)	6	LEA	43	9	1M1F
	22	Wistar	13	3	1F
		Wistar/LEA	23	9	1F
TgWW1 (XX)	6, 7	Wistar	53	9	2M7F
TgWW1 + C (XX)	8	Wistar	46	9	1M1M or F
TgWW1s (XX)	9	Wistar	35	8	1F
TgWW2* (XX)	8	Wistar	28	1	1M

F, female; M, male.
*ES cell line established by using specific serum. TgWW1 + C refers to a stable transfectant possessing CAG-AmCyan1 transgene.

cell clones that possess a correct gene expression pattern of the transgene. Our *Oct4*-Venus esTg rats will be useful for the generation of iPS cells as a pluripotency monitoring system with respect to previous work in mice (9, 18, 19). For further study, addressing the mechanism of the silencing effect on the transgenes should be crucial.

The complete generation of esTg rats might be based on the use of a culture medium containing 20% serum and YPAC, which might provide strong protectection from cell damage during gene introduction with electrical stimuli and maintain pluripotency with a stable karyotype during the cloning and expansion process. To support viability, serum was temporally used in a previous report when rat ES cells were electroporated and cultured overnight in a 2i medium (6). Such efforts are not necessary with our rat ES cells, which are tolerant to the damage induced by gene introduction because of the presence of 20% serum in the YPAC medium. Furthermore, we have confirmed that drug selection through the use of G418 is efficient in rat ES cells for generating genetically modified rats.

Previous work has suggested that the failure in the establishment of authentic rat ES cells over the past 2 decades was attributable to the presence of serum (6, 7). Indeed, serum may contain various kinds of nutrient factors as well as differentiation factors for rat ES cells (20). The reason why we succeeded in the establishment of such significant pluripotent cell lines might be attributable not only to the signaling inhibitors shielding ES cells from differentiation but to the use of the nutrients in the serum. Monitoring serum quality for better ES cell culturing is extremely important. Nevertheless, our combination of YPAC and different serum, which is used for culturing MEFs, allowed stable establishment of rat ES cell lines. Our success is thus partly attributable to the strong potential of YPAC in the maintenance of ES cells regardless of differentiation factors under different culture conditions.

It is noteworthy that leukemia inhibitory factor (LIF) was not necessary in our culture medium, although recent reports have suggested that its addition improved rat ES or rat iPS cell ability to suppress differentiation (6, 7, 10). It has been shown that LIF is the key cytokine secreted by feeders in supporting mouse ES cell self-renewal (21, 22) and that LIF was able to replace the requirement for feeders in propagation (23, 24). Ying et al. (8) demonstrated that a combination of PD0325901 and CHIR99021 enabled mouse ES cells to maintain pluripotency by substituting LIF, feeders, and serum. Considering these reports, the addition of LIF in our culture condition might be dispensable because of the inclusion of serum, MEFs, and the two inhibitors. Actually, the expression level of *Tbx3*, which is involved in mediating LIF signaling (25), was up-regulated in the rat ES cells. Moreover, we found that the expression of a suppressor of cytokine signaling 3 (*SOCS3*), which is one of the STAT3's direct target genes (26),

Table 3. Summary of germline chimeras: Chimeras and germline transmission judged by coat color of F1 pups

Cell line (gender)	Passage no.	Host blastocyst	Injected embryos	Pup no.	Chimera no.	Mating no.	Germline chimera
–YPAC injection							
TgWL1 (XX)	6–8	Wistar	226	44	1M*	0	—
+YPAC injection							
TgWL1 (XX)	11, 12	Wistar	123	23	3M5F	1M3F	1F
TgWL2 (XX)	4, 6	Wistar	70	10	2M3F	1M3F	2F
TgWW1 (XX)	9	Wistar/ LEA	79	19	5M3F	3F	1F
WW1 (XX)	10	LEA	27	7	2M1F	1F	1F
LL1 (XX)	4, 6	Wistar	107	13	3F	2F	1F
LL2 (XX)	9	Wistar	52	6	3F	3F	2F

F, female; M, male.
*Coat-color contribution is sparse (Fig. S5).

was up-regulated after stimulation with rat LIF (27) even in the YPAC medium. Thus, it seems possible to improve the culture condition further by the administration of rat LIF.

The six established ES cell lines in this work were all female. This result does not correspond to mice, because most of the mouse ES cell lines are male. In our present study, we continued to culture rat ES cell lines exhibiting rapid cell proliferation, resulting in the establishment of six female lines. Thus, we speculate that female blastocysts are suitable for the establishment of rat ES cells or that the addition of MEK and GSK3 inhibitors to the culture medium facilitates female-specific rapid cell growth in rat ES cells. A previous study using MEK and GSK3 inhibitors also reported that six of seven rat ES cell lines were female (6).

Although two groups reported the establishment of authentic rat ES cells, only one of several cell lines accomplished germline transmission in each group (6, 7). So far, there is no report of successful generation of knockout/knockin rats from ES cells. Thus, trials to produce more potent cell lines and to find the optimal combination of rat strains for donor ES cells, host blastocysts, and recipient foster female animals remain to be addressed (6, 7). In this study, our YPAC culture and injection method overcame the difficulty of completing germline transmission in all six ES cell lines independent of rat strains. The YPAC condition will enable the selection of preferable rat strains for the generation of genetically modified rats from ES cells, bringing great advantages to research for strain-specific disease models. We believe that the availability of our rat ES cells and the YPAC injection technique will also open up a valuable platform for routinely generating knockout/knockin rats, holding out the promise for generation of previously undescribed disease models.

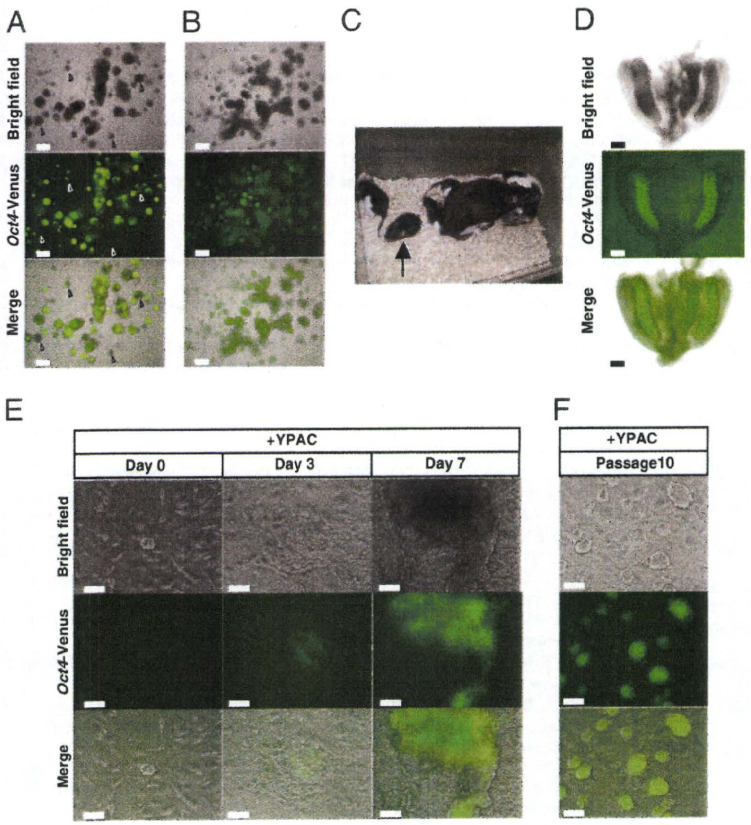

Fig. 4. Generation of Tg rats from ES cells. (*A* and *B*) Cloning and expansion of *Oct4*-Venus transfectants. An *Oct4*-Venus transgene was introduced into ES cells (LL2) at passage 5. Venus-positive clones were passaged without drug selection. (*A*) Arrowheads indicate ES cells with Venus expression silenced. (*B*) ES cells with homogeneous expression of *Oct4*-Venus. (*C*) Generation of Tg rats from ES cell clone displaying homogeneous expression of *Oct4*-Venus. An arrow indicates esTg rats through germline transmission from the chimeric rat. (*D*) Venus fluorescence in gonads of an esTg embryo at 16.0 days postcoitum (dpc). (*E*) Outgrowth of esTg blastocyst in YPAC medium. (*F*) Rat ES cell line derived from an esTg blastocyst. The expression of *Oct4*-Venus did not receive a silencing effect even after 10 passages. (Scale bars, *A*, *B*, and *D*: 300 μm; *E* and *F*: 100 μm.)

DEVELOPMENTAL BIOLOGY

Materials and Methods

Media, Feeder, Animals, and Primers. YPAC medium was prepared by the addition of the four respective inhibitors [10 μM Y-27632 (WAKO), 1 μM PD0325901 (Axon Medchem), 0.5 μM A-83-01 (TOCRIS), and 3 μM CHIR99021 (Axon Medchem)] to basic medium. The basic medium is composed of DMEM [including 110 mg/L sodium pyruvate and 200 mM GlutaMAX (GIBCO)], 20% (vol/vol) FBS (ES Cell Qualified FBS, Lot No. 1204059; GIBCO), 0.1 mM 2-mercaptoethanol (SIGMA), 1% nonessential amino acid stock (GIBCO), and 1× antibiotic antimycotic (GIBCO). Mitomycin C-treated MEFs resistant to neomycin (Millipore) were used as feeders and maintained in DMEM/10% (vol/vol) FBS (Lot No. SFB30-1502; EQUITECH-BIO, Inc.) medium with 1× antibiotic antimycotic. Animal experiments were performed in compliance with the guidelines of the Institute for Laboratory Animal Research, National Cancer Center Research Institute. The Wistar strain, LEA strain, or a hybrid of the Wistar and LEA strain was used in this work. All the primer sequences are listed in Table S1.

Generation of *Oct4*-Venus Tg Rats via a Conventional Method. The DNA fragment of the *Oct4* promoter region (3.9 kb) was obtained by PCR using KOD Version 2 DNA polymerase (Toyobo) from Wistar rat genomic DNA and was inserted into a pCS2-Venus plasmid (14). The *Oct4* promoter-Venus (*Oct4*-Venus) DNA fragment was injected into pronuclei of fertilized eggs in a Wistar rat strain (Oriental Yeast Co., Ltd.). Six Tg-positive founders were obtained from 222 injected fertilized eggs.

Establishment of Rat ES Cells from Blastocysts. Rat blastocysts were gently flushed out from the uteri of E4.5- or E5.0-timed pregnant rats with basic ES medium. After removal of the zona with acid Tyrode's solution (Ark Resource Co., Ltd.), whole blastocysts were plated onto six-well plates and cultured on MEFs in the basic ES medium with or without YPAC. After around 7 d, the blastocyst outgrowths were cut into pieces and replated under the same YPAC conditions. Emerging ES cell colonies were then dissociated using Accutase and were expanded. Established ES cell lines were routinely maintained under MEF-YPAC conditions and passaged every 3–4 d. Floated colonies were also passaged. Cells were cryopreserved and recovered by conventional procedures using YPAC medium and DMSO as a cryoprotectant. In the cell line of TgWL1 or TgWL2, 1,000 U/mL rat LIF (25) was added to the YPAC medium until passage 4 or 3, respectively.

Quantitative PCR Analysis. Total RNA was isolated using ISOGEN (Nippongene). cDNA was synthesized with 2 μg of the total RNA using Super Script III RT (Invitrogen) and oligo-dT primer (Invitrogen). cDNAs were used for PCR utilizing Platinum SYBR Green qPCR SuperMix UDG (Invitrogen). Optimization of the quantitative (q)RT-PCR was performed according to the manufacturer's instructions (PE Applied Biosystems). All quantitations were normalized to an endogenous control *GAPDH*.

ALP and Immunofluorescent Staining. Cells were fixed in 4% (wt/vol) paraformaldehyde. ALP staining was performed with Vector Blue substrate (Vector Labs) according to the manufacturer's instructions. Primary antibodies used include the following: Oct4 (C-10, 1:20; Santa Cruz), Nanog (1:20; ReproCell), and Sox2 (1:20; BioLegend). Alexa Fluor fluorescent secondary antibodies (Invitrogen) were used at a 1:500 dilution. Nuclei were visualized with DAPI staining.

Teratoma Formation. The 2.6×10^6 TgWW1 cells (passage 5) were injected under the skin of immunodeficient mice. Teratomas were obtained 34 d after the injection. They were embedded in paraffin wax and stained with H&E.

EB Formation. After ES cells were split into single cells using Accutase, they were cultured in a basal ES medium with or without three-inhibitor PAC, excluding Y-27632, on a low-cell-binding dish (NUNC). RNAs were extracted from the EBs at day 3 or 7, followed by qPCR examination.

Blastocyst Injection. The blastocysts from E4.5-timed pregnant rats were placed into 500 μL of injection medium composed of YPAC (or PAC) and basal ES cell medium without antibiotic antimycotic, and they were then incubated for 2–3 h. The well-expanded blastocysts were used for microinjection. For ES cell preparation, 10–20 domed or floated colonies were picked up by hand-made capillary and treated with an Accutase droplet for 5 min, followed by being split into single cells in a droplet of injection medium. The cells were transferred in 500 μL of the injection medium and incubated for 30–60 min at room temperature. After centrifugation, ES cells were transferred into a droplet of the injection medium under mineral oil (SIGMA). Ten to 15 ES cells were injected into each blastocyst and incubated at 37 °C for 3–5 h in the injection medium to allow the recovery of embryos. Ten to 20 embryos were then transferred into the uterine horn of each E3.5-timed pseudopregnant female rat. Chimeric rats were identified by coat color. Germline transmission was confirmed by the F1 rat coat color resulting from mating of chimera or *Oct4*-Venus fluorescence in germ cells in the fetal gonad. Genotyping of animals was carried out by PCR on tail DNA.

Gene Transfection of Rat ES Cells. For nucleofection, 5 μg of CAG-AmCyan1 or 10 μg of *Oct4*-Venus plasmid linearized by SalI was transfected into 3.2×10^6 TgWW1 or 3×10^6 LL2 rat ES cells, respectively, using a Mouse ES Cell Nucleofector Kit (Amaxa, Inc.). The cells were plated on MEFs in the YPAC medium with 2% (vol/vol) matrigel (BD Biosciences). Three combined colonies of CAG-AmCyan1 or a single colony of *Oct4*-Venus transfectant, positive for cyan or green fluorescence, respectively, was picked up by hand-made capillary and expanded without drug selection.

ACKNOWLEDGMENTS. We thank Shinobu Ueda, Takumi Teratani, Yoshitaka Tamai, and Taku Shimizu for technical advice; Luc Gailhouste for comments on the manuscript; Atsushi Miyawaki (RIKEN) for pCSII-Venus plasmid; Katsuyuki Hayashi and DNA Chip Research, Inc., for microarray analysis; and Setsuo Hirohashi and Masaaki Terada for great support of our project. This work was supported by a Grant-in-Aid for the Third-Term Comprehensive 10-Year Strategy for Cancer Control.

1. Jacob HJ (1999) Functional genomics and rat models. *Genome Res* 9:1013–1016.
2. Liao J, et al. (2009) Generation of induced pluripotent stem cell lines from adult rat cells. *Cell Stem Cell* 4:11–15.
3. Iannaccone PM, Jacob HJ (2009) Rats!. *Dis Model Mech* 2:206–210.
4. Geurts AM, et al. (2009) Knockout rats via embryo microinjection of zinc-finger nucleases. *Science* 325:433.
5. Ueda S, et al. (2008) Establishment of rat embryonic stem cells and making of chimera rats. *PLoS ONE* 3:e2800.
6. Buehr M, et al. (2008) Capture of authentic embryonic stem cells from rat blastocysts. *Cell* 135:1287–1298.
7. Li P, et al. (2008) Germline competent embryonic stem cells derived from rat blastocysts. *Cell* 135:1299–1310.
8. Ying QL, et al. (2008) The ground state of embryonic stem cell self-renewal. *Nature* 453:519–523.
9. Silva J, et al. (2008) Promotion of reprogramming to ground state pluripotency by signal inhibition. *PLoS Biol* 6:e253.
10. Li W, et al. (2009) Generation of rat and human induced pluripotent stem cells by combining genetic reprogramming and chemical inhibitors. *Cell Stem Cell* 4:16–19.
11. Lin TA, et al. (2009) A chemical platform for improved induction of human iPSCs. *Nat Methods* 6:805–808.
12. Ishizaki T, et al. (2000) Pharmacological properties of Y-27632, a specific inhibitor of rho-associated kinases. *Mol Pharmacol* 57:976–983.
13. Watanabe K, et al. (2007) A ROCK inhibitor permits survival of dissociated human embryonic stem cells. *Nat Biotechnol* 25:681–686.
14. Nagai T, et al. (2002) A variant of yellow fluorescent protein with fast and efficient maturation for cell-biological applications. *Nat Biotechnol* 20:87–90.
15. Chew JL, et al. (2005) Reciprocal transcriptional regulation of Pou5f1 and Sox2 via the Oct4/Sox2 complex in embryonic stem cells. *Mol Cell Biol* 25:6031–6046.
16. Yeom YI, et al. (1996) Germline regulatory element of Oct-4 specific for the totipotent cycle of embryonal cells. *Development* 122:881–894.
17. Keller GM (1995) In vitro differentiation of embryonic stem cells. *Curr Opin Cell Biol* 7:862–869.
18. Huangfu D, et al. (2008) Induction of pluripotent stem cells by defined factors is greatly improved by small-molecule compounds. *Nat Biotechnol* 26:795–797.
19. Esteban MA, et al. (2010) Vitamin C enhances the generation of mouse and human induced pluripotent stem cells. *Cell Stem Cell* 6:71–79.
20. Kawamata M, Ochiya T (2010) Establishment of embryonic stem cells from rat blastocysts. *Methods Mol Biol* 597:169–177.
21. Evans MJ, Kaufman MH (1981) Establishment in culture of pluripotential cells from mouse embryos. *Nature* 292:154–156.
22. Martin GR (1981) Isolation of a pluripotent cell line from early mouse embryos cultured in medium conditioned by teratocarcinoma stem cells. *Proc Natl Acad Sci USA* 78:7634–7638.
23. Smith AG, et al. (1988) Inhibition of pluripotential embryonic stem cell differentiation by purified polypeptides. *Nature* 336:688–690.
24. Williams RL, et al. (1988) Myeloid leukaemia inhibitory factor maintains the developmental potential of embryonic stem cells. *Nature* 336:684–687.
25. Niwa H, Ogawa K, Shimosato D, Adachi K (2009) A parallel circuit of LIF signalling pathways maintains pluripotency of mouse ES cells. *Nature* 460:118–122.
26. Burdon T, Chambers I, Stracey C, Niwa H, Smith A (1999) Signaling mechanisms regulating self-renewal and differentiation of pluripotent embryonic stem cells. *Cells Tissues Organs* 165:131–143.
27. Takahama Y, et al. (1998) Molecular cloning and functional analysis of cDNA encoding a rat leukemia inhibitory factor: Towards generation of pluripotent rat embryonic stem cells. *Oncogene* 16:3189–3196.

18. O. Golonzhka *et al.*, *J. Invest. Dermatol.* **129**, 1459 (2009).
19. See supporting material on *Science* Online.
20. R. S. Welner *et al.*, *Blood* **109**, 4825 (2007).
21. C. A. Vosshenrich *et al.*, *J. Exp. Med.* **204**, 2569 (2007).
22. W. Dontje *et al.*, *Blood* **107**, 2446 (2006).
23. H. Shigematsu *et al.*, *Immunity* **21**, 43 (2004).
24. C. H. Martin *et al.*, *Nat. Immunol.* **4**, 866 (2003).
25. H. Takatori *et al.*, *J. Exp. Med.* **206**, 35 (2009).
26. C. A. Vosshenrich *et al.*, *Nat. Immunol.* **7**, 1217 (2006).
27. D. M. Gascoyne *et al.*, *Nat. Immunol.* **10**, 1118 (2009).
28. S. Doulatov *et al.*, *Genes Dev.* **23**, 2076 (2009).
29. A. P. Weng *et al.*, *Genes Dev.* **20**, 2096 (2006).
30. M. Ciofani, J. C. Zúñiga-Pflücker, *Immunol. Res.* **34**, 117 (2006).
31. M. Ciofani, G. C. Knowles, D. L. Wiest, H. von Boehmer, J. C. Zúñiga-Pflücker, *Immunity* **25**, 105 (2006).
32. G. Bain, W. J. Romanow, K. Albers, W. L. Havran, C. Murre, *J. Exp. Med.* **189**, 289 (1999).
33. T. Kreslavsky *et al.*, *Proc. Natl. Acad. Sci. U.S.A.* **106**, 12453 (2009).
34. We thank P. Liu, H. Kawamoto, P. Li, T. Ikawa, D. Scripture-Adams, and members of the Rothenberg lab for sharing unpublished results and helpful discussion; D. Metzger and J.-M. Bornert for help with generation of the floxed Bcl11b mice; H.-Y. Kueh for guidance in data analysis; T. Taghon and F. Costantini for vectors and mice; D. Perez and R. Diamond for flow cytometry support; and R. Butler and S. Washburn for animal care and breeding supervision. Supported by a California Institute for Regenerative Medicine fellowship (L.L.), NIH grants R33 HL089123 and RC2 CA148278 (E.V.R.), NIH grant R01 GM60852 (M.L.), the Caltech–City of Hope Biomedical Initiative, the Louis Garfinkle Memorial Laboratory Fund, the Al Sherman Foundation, and the A. B. Ruddock Professorship.

Supporting Online Material

www.sciencemag.org/cgi/content/full/329/5987/89/DC1
Materials and Methods
SOM Text
Figs. S1 to S11
Tables S1 and S2
References

2 March 2010; accepted 19 May 2010
10.1126/science.1188989

An Essential Developmental Checkpoint for Production of the T Cell Lineage

Tomokatsu Ikawa,[1] Satoshi Hirose,[2] Kyoko Masuda,[1] Kiyokazu Kakugawa,[1] Rumi Satoh,[1] Asako Shibano-Satoh,[1] Ryo Kominami,[2] Yoshimoto Katsura,[1,3] Hiroshi Kawamoto[1]*

In early T cell development, progenitors retaining the potential to generate myeloid and natural killer lineages are eventually determined to a specific T cell lineage. The molecular mechanisms that drive this determination step remain unclarified. We show that, when murine hematopoietic progenitors were cultured on immobilized Notch ligand DLL4 protein in the presence of a cocktail of cytokines including interleukin-7, progenitors developing toward T cells were arrested and the arrested cells entered a self-renewal cycle, maintaining non-T lineage potentials. Reduced concentrations of interleukin-7 promoted T cell lineage determination. A similar arrest and self-renewal of progenitors were observed in thymocytes of mice deficient in the transcription factor Bcl11b. Our study thus identifies the earliest checkpoint during T cell development and shows that it is Bcl11b-dependent.

T cells are generated from multipotent hematopoietic stem cells through a series of differentiation steps. The first step in this pathway is the generation of progenitors that have lost erythroid/megakaryocyte potential but retain the capacity to generate other hemopoietic cells, including myeloid, T, and B cells (*1*–*6*). We and others have recently identified the next stage, in which the T cell progenitors have lost B cell potential but are still able to generate myeloid cells, dendritic cells (DCs), and natural killer (NK) cells (*7*, *8*). Therefore, the most critical step for development of the T cell lineage is now thought to be at the point where myeloid potential is terminated.

We sought to identify the step at which progenitors become fully committed to the T cell lineage and what regulates this transition. A reliable way to substantiate that a given step is critical for the development of a lineage is to demonstrate developmental arrest at the stage before that step under particular conditions. In the case of B cell differentiation, deletion of *E2a*, *Ebf*, or *Pax5* genes leads to an early developmental arrest before formation of a functional *IgH* chain gene; these arrested B cell progenitors undergo self-renewal and remain B lineage uncommitted, with the potential to develop along other lineages, including myeloid and T cell (*9*–*11*). This case illustrates that such a critical developmental checkpoint exists at the step when uncommitted B cell progenitors become determined to the B cell lineage. Unlike the B cell lineage, to date no such checkpoint has been identified for the T cell lineage before the initiation of *TCR* gene rearrangement.

As T cell progenitors develop, they proceed through developmental stages referred to as DN1 to DN4 (double-negative $CD4^-CD8^-$) that can be tracked by surface phenotype. The DN2 stage can be subdivided into two stages based on transgenic green fluorescent protein (GFP) expression controlled by the proximal lck (plck) promoter (lck is a src family kinase selectively expressed by T cells). GFP^- cells retain non-T lineage potential, including that for myeloid cells, DCs, and NK cells, whereas the latter stage GFP^+ cells are determined to the T cell lineage (*7*, *12*). We designate these two stages DN2mt (myeloid-T) and DN2t (T-lineage determined) and term the step between these stages the DN2-determination step. This determination step is thought to be the first critical checkpoint in T cell development (*13*).

We cultured lineage-negative (Lin^-) c-kit^+ Sca-1^+ (LKS) cells from 13 days post-coitum (dpc) murine fetal liver with immobilized Delta-like 4 (DLL4) protein in the presence of the cytokines SCF (stem cell factor), Flt3L (FMS-like tyrosine kinase ligand), and interleukin (IL)–7 (fig. S1). After 7 days of culture, cells remained at the DN stage (Fig. 1A, left panel), whereas in the control group, where cells were cultured with TSt-4 stromal cells expressing DLL4 (TSt-4/DLL4), generation of $CD4^+CD8^+$ double-positive (DP) cells was observed (fig. S2). Upon closer analysis on DN cells generated in the feeder-free condition, we observed that these cells resembled DN2mt cells (maintained c-$kit^{high}CD25^+$) (Fig. 1A, right panel) and thus named them FFDN2 cells (feeder-free-cultured DN2-like cells). By several criteria, the FFDN2 cells appeared identical to DN2mt cells: (i) they gave rise to authentic αβ T cells when transferred to a TSt-4/DLL4 stromal coculture system (fig. S3, A and B); (ii) they retained the potential to produce macrophages (Fig. 1B), NK cells, and DCs (fig. S3, C and D); (iii) intracellular T cell receptor (TCR) β chain protein was not expressed (Fig. 1C); and (iv) their gene expression profiles were similar to those of DN2mt cells (Fig. 1D and fig. S4). Furthermore, GFP expression was not observed in FFDN2 cells generated from progenitors isolated from plck-GFP mice (Fig. 1E). It is unlikely that this arrest is due to the failure of TCR gene rearrangement because enforced expression of a functional TCRβ chain gene did not prevent the developmental arrest (fig. S5). FFDN2 cells could not generate B cells (fig. S3E), indicating that dedifferentiation to more primitive progenitors did not occur in this culture system. Of note, FFDN2 cells showed an almost unlimited in vitro expansion (Fig. 1F), while essentially maintaining c-kit and CD25 expression (Fig. 1G) and a developmental potential comparable to that of freshly isolated DN2mt cells (fig. S6). Cells in the c-kit^+CD25^+ fraction possessed the potential to maintain long-term culture, because long-term culture could be maintained by using c-kit^+CD25^+ cells at the time of passage (fig. S7). Such self-renewal capacity, together with our other results,

[1]Laboratory for Lymphocyte Development, RIKEN Research Center for Allergy and Immunology, Yokohama 230-0045, Japan. [2]Department of Molecular Genetics, Graduate School of Medical and Dental Sciences, Niigata University, Niigata 951-8510, Japan. [3]Division of Cell Regeneration and Transplantation, Advanced Medical Research Center, Nihon University School of Medicine, Tokyo 173-8610, Japan.

*To whom correspondence should be addressed. E-mail: kawamoto@rcai.riken.jp

indicated that the DN2-determination step may be a critical checkpoint for T cell development.

To investigate the molecular mechanisms of T cell lineage determination, we searched for an environmental cue that could drive the arrested cells through the DN2-determination step. After testing various cytokines and Notch ligand conditions in the feeder-free culture system, we found that FFDN2 cells initiate differentiation when the concentration of IL-7 is reduced on day 7 of culture (10 ng/ml to 1 ng/ml). In this induction system, GFP^+ DN3 cells appear on day 3 after IL-7 reduction (Fig. 2A). These cells did not express myeloid-lineage transcription factors *PU.1* (*Sfpi1*) and *C/EBPα*, whereas T cell lineage–associated genes such as *lck*, *Tcf1*, *pTα*, and *Bcl11b* were markedly up-regulated (Fig. 2B). Notably, cells in these cultures developed up to the αβTCR-

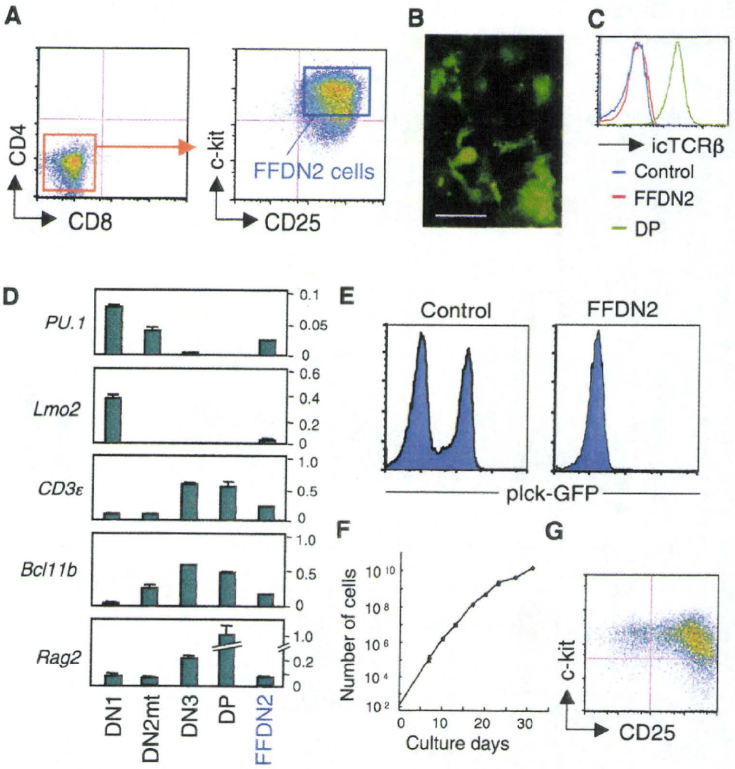

Fig. 1. Immobilized DLL4 with a combination of cytokines induces self-renewing expansion of immature thymocytes. (**A**) LKS progenitor cells (200 cells) from 13 dpc murine fetal liver were cultured with immobilized Fc-DLL4 supplemented with 10 ng/ml of SCF, IL-7, and Flt3L for 7 days. Generated cells were harvested and stained with the indicated antibodies and analyzed by a flow cytometry. Data are representative of four independent experiments. (**B**) A photomicrograph of macrophages generated from FFDN2 cells. FFDN2 cells induced from green mouse progenitors in a similar manner as (A) were sorted and cultured with TSt-4 stromal cells for 14 days in the presence of 10 ng/ml M-CSF (macrophage colony-stimulating factor). Macrophages are seen as large GFP^+ cells. Scale bar, 100 μm. (**C**) Expression of intracellular (ic) TCRβ in FFDN2 cells, in negative control cells generated in feeder-free culture using only the Fc portion (Control), and in positive control $CD4^+CD8^+$ DP cells from an adult thymus. (**D**) mRNA expression of lineage-specific genes in cells derived from DN1, DN2mt, DN3, DP, and FFDN2 cells determined by quantitative reverse transcription polymerase chain reaction (RT-PCR). Expression was normalized to acidic ribosomal protein (ARP) mRNA expression, and the mean + SD of triplicate samples is shown. Data are representative of three independent experiments. (**E**) Flow cytometric analysis of GFP expression in FFDN2 cells generated from progenitors of plck-GFP mice in comparison with cells generated under TSt-4/DLL4 conditions (Control). Data are representative of three independent experiments. (**F**) A growth curve of FFDN2 cells. Viable cells were enumerated at the indicated time points. (**G**) c-kit versus CD25 expression by FFDN2 cells after long-term culture. Fetal liver LKS cells were cultured under feeder (–) conditions for 30 days and then analyzed by flow cytometry. Data are representative of four independent experiments.

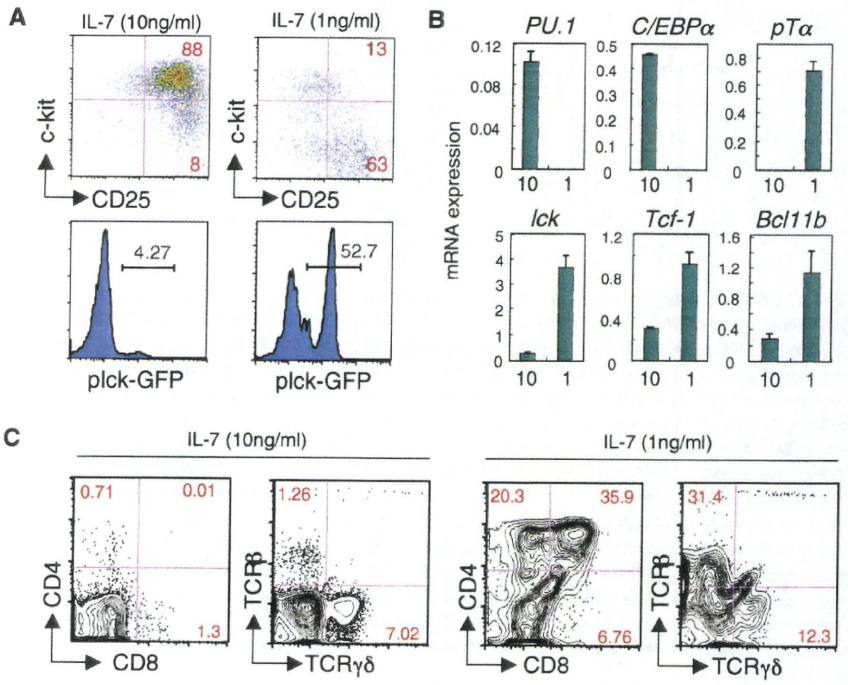

Fig. 2. Reduction of IL-7 concentration induces the generation of DP cells in feeder-free culture. (**A**) LKS cells (200 cells) from 13 dpc fetal liver were cultured with immobilized Fc-DLL4 in the presence of SCF, IL-7, and Flt3L (10 ng/ml). After 7 days, the concentration of IL-7 was maintained or reduced to 1 ng/ml, and the cells were cultured for an additional 3 days. Cells were analyzed by flow cytometry. Data are representative of three independent experiments. (**B**) mRNA expression of lineage-associated genes in cells cultured in the presence of 10 ng/ml or 1 ng/ml of IL-7 in the same manner as (A). Expression was normalized to ARP mRNA expression, and the mean + SD of triplicate samples is shown. Data are representative of three independent experiments. (**C**) Flow cytometric analysis of cells generated 7 days after switching to cultures with either high or low IL-7 concentration. Cells were analyzed for the expression of CD4 versus CD8 and TCRβ versus TCRγδ. Data are representative of five independent experiments.